ISSN 2644-3260 (online)

Artificial Intelligence in *Medical Imaging*

Artif Intell Med Imaging 2021 April 28; 2(2): 13-55

Published by Baishideng Publishing Group Inc

AIMI

Artificial Intelligence in Medical Imaging

Contents

Bimonthly Volume 2 Number 2 April 28, 2021

MINIREVIEWS

Artificial Intelligence in Medical Imaging

Bimonthly Volume 2 Number 2 April 28, 2021

Contents

ABOUT COVER

Editorial Board Member of *Artificial Intelligence in Medical Imaging*, Guo-Lin Ma, MD, PhD, Professor, Department of Radiology, China-Japan Friend Hospital, Beijing 100029, China. maguolin1007@qq.com

AIMS AND SCOPE

The primary aim of *Artificial Intelligence in Medical Imaging* (*AIMI*, *Artif Intell Med Imaging*) is to provide scholars and readers from various fields of artificial intelligence in medical imaging with a platform to publish high-quality basic and clinical research articles and communicate their research findings online.

AIMI mainly publishes articles reporting research results obtained in the field of artificial intelligence in medical imaging and covering a wide range of topics, including artificial intelligence in radiology, pathology image analysis, endoscopy, molecular imaging, and ultrasonography.

INDEXING/ABSTRACTING

There is currently no indexing.

RESPONSIBLE EDITORS FOR THIS ISSUE

Production Editor: *Yan-Xia Xing*; **Production Department Director:** *Yun-Xiaojian Wu*; **Editorial Office Director:** *Yun-Xiaojiao Wu*.

NAME OF JOURNAL
Artificial Intelligence in Medical Imaging

ISSN
ISSN 2644-3260 (online)

LAUNCH DATE
June 28, 2020

FREQUENCY
Bimonthly

EDITORS-IN-CHIEF
Xue-Li Chen, Caroline Chung, Jun Shen

EDITORIAL BOARD MEMBERS
https://www.wjgnet.com/2644-3260/editorialboard.htm

PUBLICATION DATE
April 28, 2021

COPYRIGHT
© 2021 Baishideng Publishing Group Inc

INSTRUCTIONS TO AUTHORS
https://www.wjgnet.com/bpg/gerinfo/204

GUIDELINES FOR ETHICS DOCUMENTS
https://www.wjgnet.com/bpg/GerInfo/287

GUIDELINES FOR NON-NATIVE SPEAKERS OF ENGLISH
https://www.wjgnet.com/bpg/gerinfo/240

PUBLICATION ETHICS
https://www.wjgnet.com/bpg/GerInfo/288

PUBLICATION MISCONDUCT
https://www.wjgnet.com/bpg/gerinfo/208

ARTICLE PROCESSING CHARGE
https://www.wjgnet.com/bpg/gerinfo/242

STEPS FOR SUBMITTING MANUSCRIPTS
https://www.wjgnet.com/bpg/GerInfo/239

ONLINE SUBMISSION
https://www.f6publishing.com

© 2021 Baishideng Publishing Group Inc. All rights reserved. 7041 Koll Center Parkway, Suite 160, Pleasanton, CA 94566, USA
E-mail: bpgoffice@wjgnet.com https://www.wjgnet.com

Artificial Intelligence in Medical Imaging

Submit a Manuscript: https://www.f6publishing.com

Artif Intell Med Imaging 2021 April 28; 2(2): 13-31

DOI: 10.35711/aimi.v2.i2.13

ISSN 2644-3260 (online)

MINIREVIEWS

Artificial intelligence in radiation oncology

Melek Yakar, Durmus Etiz

ORCID number: Melek Yakar 0000-0002-9042-9489; Durmus Etiz 0000-0002-2225-0364.

Author contributions: Yakar M and Etiz D collected data and wrote the manuscript; Etiz D formatted and revised the article.

Conflict-of-interest statement: The authors declare that they have no conflicts of interest.

Open-Access: This article is an open-access article that was selected by an in-house editor and fully peer-reviewed by external reviewers. It is distributed in accordance with the Creative Commons Attribution NonCommercial (CC BY-NC 4.0) license, which permits others to distribute, remix, adapt, build upon this work non-commercially, and license their derivative works on different terms, provided the original work is properly cited and the use is non-commercial. See: http://creativecommons.org/Licenses/by-nc/4.0/

Manuscript source: Invited manuscript

Specialty type: Oncology

Country/Territory of origin: Turkey

Peer-review report's scientific quality classification

Grade A (Excellent): 0

Grade B (Very good): B

Melek Yakar, Durmus Etiz, Department of Radiation Oncology, Eskisehir Osmangazi University Faculty of Medicine, Eskisehir 26040, Turkey

Melek Yakar, Durmus Etiz, Center of Research and Application for Computer Aided Diagnosis and Treatment in Health, Eskisehir Osmangazi University, Eskisehir 26040, Turkey

Corresponding author: Melek Yakar, MD, Assistant Professor, Department of Radiation Oncology, Eskisehir Osmangazi University Faculty of Medicine, Büyükdere, Meselik Campus, Eskisehir 26040, Turkey. mcakcay@ogu.edu.tr

Abstract

Artificial intelligence (AI) is a computer science that tries to mimic human-like intelligence in machines that use computer software and algorithms to perform specific tasks without direct human input. Machine learning (ML) is a subunit of AI that uses data-driven algorithms that learn to imitate human behavior based on a previous example or experience. Deep learning is an ML technique that uses deep neural networks to create a model. The growth and sharing of data, increasing computing power, and developments in AI have initiated a transformation in healthcare. Advances in radiation oncology have produced a significant amount of data that must be integrated with computed tomography imaging, dosimetry, and imaging performed before each fraction. Of the many algorithms used in radiation oncology, has advantages and limitations with different computational power requirements. The aim of this review is to summarize the radiotherapy (RT) process in workflow order by identifying specific areas in which quality and efficiency can be improved by ML. The RT stage is divided into seven stages: patient evaluation, simulation, contouring, planning, quality control, treatment application, and patient follow-up. A systematic evaluation of the applicability, limitations, and advantages of AI algorithms has been done for each stage.

Key Words: Radiation oncology; Radiotherapy; Artificial intelligence; Deep learning; Machine learning

©The Author(s) 2021. Published by Baishideng Publishing Group Inc. All rights reserved.

Core Tip: Beginning with the initial patient interview, artificial intelligence (AI) can help predict posttreatment disease prognosis and toxicity. Additionally, AI can assist in

Grade C (Good): 0
Grade D (Fair): 0
Grade E (Poor): 0

Received: March 4, 2021
Peer-review started: March 4, 2021
First decision: March 14, 2021
Revised: March 30, 2021
Accepted: April 20, 2021
Article in press: April 20, 2021
Published online: April 28, 2021

P-Reviewer: Lee KS
S-Editor: Wang JL
L-Editor: Filipodia
P-Editor: Xing YX

the automated segmentation of both the organs at risk and target volumes and the treatment planning process with advanced dose optimization. AI can optimize the quality control process and support increased safety, quality, and maintenance efficiency.

Citation: Yakar M, Etiz D. Artificial intelligence in radiation oncology. *Artif Intell Med Imaging* 2021; 2(2): 13-31
URL: https://www.wjgnet.com/2644-3260/full/v2/i2/13.htm
DOI: https://dx.doi.org/10.35711/aimi.v2.i2.13

INTRODUCTION

Artificial intelligence (AI) is a computer science branch that tries to imitate human-like intelligence in machines using computer software and algorithms without direct human input to perform certain tasks[1,2]. Machine learning (ML) is a subunit of AI that uses data-driven algorithms that learn to imitate human behavior based on previous example or experience[3]. Deep learning (DL) is an ML technique that uses deep neural networks to create a model. Increasing computing power and reduction of financial barriers led to the emergence of the domain of DL[4]. The growth and sharing of data, increasing computing power, and developments in AI have initiated a transformation in healthcare services. Advances in radiation oncology, clinical and dosimetric information from increasing cases, and computed tomography (CT) imaging before each fraction have resulted in the accumulation of a significant amount of information in big databases.

Evidence-based medicine is based on randomized controlled trials designed for large patient populations. However, the increasing number of clinical and biological parameters that need to be investigated makes it difficult to design studies[5]. New approaches are required for all patient populations. Clinicians should use all diagnostic tools, such as medical imaging, blood testing, and genetic testing, to decide on the appropriate combination of treatments (*e.g.*, radiotherapy, chemotherapy, targeted therapy, and immunotherapy). There are a number of individual differences that are responsible for each patient's disease or associated with response to treatment and clinical outcome. The concept of personalized treatment is based on determining and using these factors for each patient[6]. Integrating such a large amount of heterogeneous of data and producing accurate models may present difficulties and subjective individual differences for the human brain from time to time.

Beginning with the initial patient interview, AI can help predict posttreatment disease prognosis and toxicity. Additionally, AI can assist in the automated segmentation of both the organs at risk and target volume and the treatment planning process, with advanced dose optimization. AI can optimize the quality control (QA) process and support increased safety, quality, and maintenance efficiency.

The aim of this review is to summarize the radiotherapy (RT) process in workflow order by identifying specific areas where quality and efficiency can be improved with AI. The RT stage is divided into seven stages: patient evaluation, simulation, contouring, planning, QA, treatment application, and patient follow-up, and the flow chart is given in Figure 1. A systematic evaluation of the applicability, limitations, and advantages of AI algorithms has been made to each stage.

CLINICAL EVALUATION

Clinical radiation therapy workflow begins with patient assessment. This step typically includes a series of consultations including reviews of the radiation oncologist on the patient's symptoms, medical history, physical examination, pathological and genomic data, diagnostic studies of prognosis, comorbidities, and risk of toxicity from RT. The radiation oncologist then suggests a treatment plan based on the synthesis of these data. For clinicians involved in this process, the accumulation of big data beyond what people can quickly interpret is the biggest challenge[7]. AI-based methods that can be used in routine functioning may be important decision support tools for clinicians in the future. Such AI-based models have been reported to

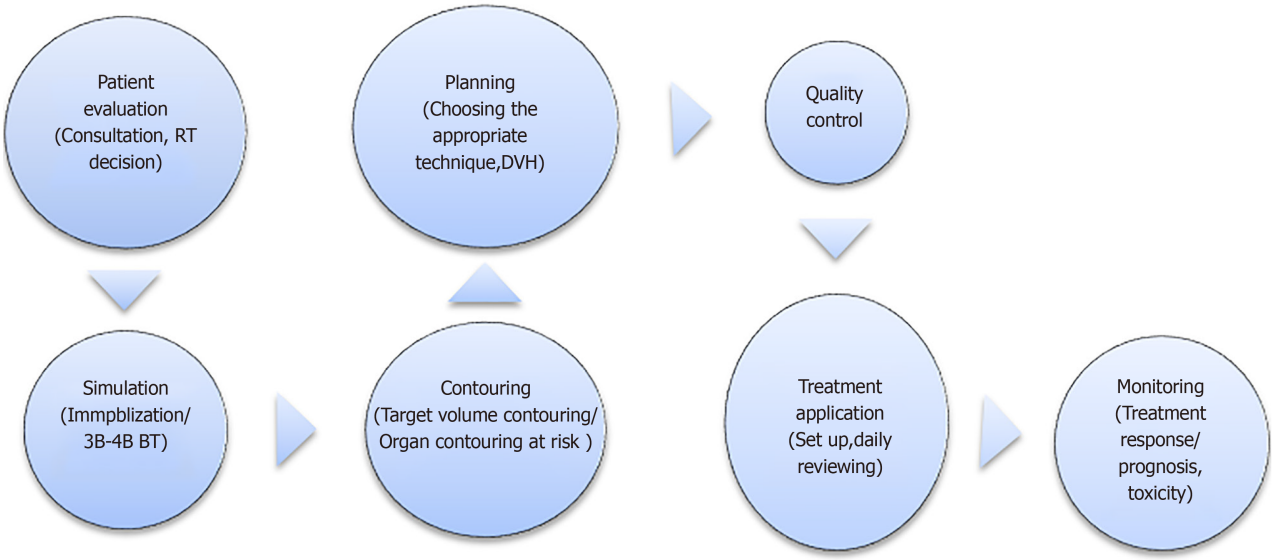

Figure 1 Workflow in radiation oncology. DVH: Dose value histogram; RT: Radiotherapy.

improve prognosis and predict treatment outcomes, but are not yet used in routine clinical practice[8].

The recent implementation of electronic health records has significantly increased the clinical documentation burden of physicians. The notes having constituted 34%-78% of physicians' working days, for each hour a physician spends in direct contact with the patient, he spends an additional 2 h in front of the computer[9]. AI solutions have the potential to automate structured documentation. They can save time requirements that add to the documentation burden, reduce burnout, protect confidentiality, and organize medical data into searchable and available items[10]. In addition, an AI-supported electronic record system may have pre-consultation and disease pre-diagnosis power, by including a timeline and the outcomes of relevant tests, procedures, and treatments from various sources[10]. AI-based systems can record patient-doctor conversations and use speech recognition and natural language processing to create a coherent narrative. Such an AI-based system does not yet exist, significant technical advances for clinical and persuasive speech require the learning of hours of selected recording of patient speech[11]. According to patient demands AI systems can present information to the patient at low, medium, or high complexity levels.

The radiation oncologist should consider many factors during the evaluation of the patient and include consideration of their interactions when making treatment decisions. At this point, data-based forecasting models can guide the doctor and make the decision phase faster and more accurate. For example, when a patient diagnosed with lung cancer is being evaluated for stereotactic RT, the patient's respiratory functions, lung capacity, tumor size, proximity of the tumor to critical organs, comorbid diseases, and performance of the patient will affect both treatment response and toxicity. If modeling is made with these and similar factors, response and toxicity rates can be determined before starting treatment. In a case with a diagnosis of left breast cancer and treatment with breast-conserving surgery, modeling created with the patient and treatment characteristics can be predicted whether she can benefit from a breath-holding technique. Big data are needed to create these estimation models. The transition to the use of AI will also increase collaboration between centers in the data collection phase and make treatments more standardized. In addition, depending on the distribution of technology in the centers in the country, AI can direct patients to appropriate treatment centers. For example, it can direct pediatric cases requiring proton therapy to a specialized center, and cases requiring palliative treatment to a conventional center).

SIMULATION

After the RT decision is made, a good simulation is required to choose the right

treatment. Immobilization technique, scanning range, and the treatment area should be accurately determined. Preliminary preparations such as use of fiducial markers for simulation, full/empty bladder, whether an empty rectum is required, renal function tests, and fasting status should be carefully considered if intravenous contrast is to be applied. Accurate and good simulation is essential to obtain a high-quality, robust treatment plan for the patient. In clinical practice, it is not uncommon to repeat a CT during CT simulation because of deficiencies and inaccuracies such as insufficient scanning range, inadequate/incorrect immobilization technique, an inappropriate level of bladder/rectum content, and hardware-related artifacts[12]. There are many questions that can be answered with AI to improve overall workflow efficiency. For example, will the patient benefit from the use of an intravenous contrast agent? Which immobilization technique should be used? Is 4-dimensional (4D)-CT simulation necessary?

Depending on the location of the disease, this process can be very complex, and optimal patient immobilization is individual, so this process often requires the participation of a radiation oncologist and a medical physicist. For example, special care should be taken to assess potential interference between the immobilization device and treatment beam angles, or patient-specific problems that could cause collisions with the RT device. In simulation, CT is still used in many centers, but brain and prostate tumors can be seen better with magnetic resonance (MR). As a solution, efforts have been made to develop CT scans using MR data, also called synthetic CT (sCT) scans using the atlas-based, sparse coding-based, or learning-based methods. Convolutional neural networks (CNNs), which are less time consuming and more efficient AI-based method with fewer artifacts, increasingly used to convert MR data to sCT[13]. Therefore, in the future, sCT scans with AI-based methods may compensate for the need for CT scanning, as they can be created with electron density data faster and are more reliable for plan generation than MR. Compared with traditional sCT methods, DL methods can be fully automated. Training with MR-CT images has been improved by the use of cycle-consistent generative adversarial networks (GANs)[14]. GANs require a new DL algorithm using two networks, a generator network creates realistic images and a differential mesh distinguishes between real and created images[14]. Studies have reported that images created by sCT and DL are accurate enough for dose calculation[15,16]. The same method can be used for other image syntheses. For example, virtual 4D-MR images can be synthesized from 4D-BT in order to see liver tumors well in image-guided RT (IGRT)[17].

Simulation is one of the most important steps in RT because ant deficiencies or errors that occur are reflected in the entire treatment process. AI techniques can be used to increase the accuracy of the simulation, to personalize it according to the patient characteristics, and to better characterize the tumor, but more studies are needed for its routine clinical use.

IMAGE REGISTRATION - SEGMENTATION

Image registration

Image registration is the process of spatially aligning two or more sets of images of the same region shot in different modalities at different times[17]. Commercially available automated image registration algorithms are typically designed to perform well only with modality-specific registration problems and require additional manual adjustments to achieve a clinically acceptable registration[7]. The two main registration methods used in RT are density based and have rigid registration. In a review of image registration Viergever *et al*[18] examined relevant developments between 1998 and 2016. They stated that DL approaches to registration can be novel game-changers in facilitating the implementation process and doing more, and they advocated the application of DL concepts to make it a routine integral part of the entire clinical imaging spectrum[18]. AI tools are also trained to determine the sequence of motion actions that result in optimal registration. These algorithms can provide better accuracy than various state-of-the-art registration methods and can be generalized to multiple display methods[19]. AI approaches have been shown to mitigate the effects of image artifacts like metal screws, guide wires, prostheses, and motion artifacts, which pose difficulties in both registration and segmentation[7].

Segmentation

In the standard workflow, the target volume and organs at risk (OARs) are manually

contoured by the radiation oncologist in a cross-section. As a result, the process is long and has a high degree of variability as a result of individual differences[20]. Manual segmentation directly affects the quality of the treatment plan and dose distribution for OARs[21]. There have been some attempts at automatic segmentation. It is the most widely available atlas-based segmentation in clinical use. First, the target image is matched with one or more selected reference images. Then, the contours in the reference image are transferred to the target image[22]. Atlas-based methods depend on the choice of atlas and the accuracy of reference images[23]. AI can be used to minimize the differences between physicians and to shorten the duration of this step in RT planning.

Segmentation of at-risk organs: To protect at-risk organs and to correctly evaluate RT toxicity, the segmentation of OARs should be done correctly. To fully benefit from technological developments in RT planning and devices, at-risk organs must be identified correctly. In clinics with high patient density, this step can be rate limiting. In addition, there may be differences among the practitioners, and because of significant anatomical changes (*e.g.*, edema, tumor response, weight loss, and others) during treatment, a new plan with new segmentation may be required. AI, particularly CNN, is a potential tool to reduce physician workload and define a standard segmentation. In recent years, DL methods have been widely used in medical applications such as organ segmentation in CNN, head-neck, lung, brain, and prostate cancers[24-27].

In a head and neck cancer study by Ibragimov *et al*[28] contouring the spinal cord, mandible, parotid glands, submandibular glands, larynx, pharynx, eyes, optic nerves, and optic chiasm was done in 50 patients by DL using CT images. They obtained dice similarity coefficients (DSCs) of between 37.4% (optic chiasm) and 89.5% (mandible). Compared with the contouring algorithm of current commercial software, contouring of the medulla spinalis, mandibular and parotid glands, larynx, pharynx, and eye globes, was better and that of the optic nerve, submandibular gland (SMG), and the optic chiasm was worse with DL. CT images were used in that study, and higher accuracy rates were achieved with MR image support[28]. In a study of head and neck organ segmentation in 200 patients with oropharyngeal squamous cell carcinoma, Chan *et al*[29] used CT for planning, with 160 cases used for training, 20 for internal validation, and 20 for testing. Mandibula, right and left parotid glands, oral cavity, brainstem, larynx, esophagus, right and left SMG, right and left temporomandibular joints were contoured. In a lifelong learning-based CNN (LL-CNN) comparison, manual contouring was used as the gold standard and DSC and root-mean-square error (RMSE) was used for accuracy. LL-CNN was then compared to 2D U-Net, 3D U-Net, single-task CNN (ST-CNN) and multitask CNN. Higher DSC and lower RMSE were obtained with LL-CNN compared with the other algorithms. The study found that LL-CNN had a better prediction accuracy than all alternative algorithms for the head and neck organs at risk[29]. In another study, Rooij *et al*[30] used CT images of 157 head and neck cancer patients, 142 for case training and 15 for testing. The right and left SMGs, right and left parotid glands, larynx, cricopharynx, pharyngeal constrictor muscle, upper esophageal sphincter, brain stem, oral cavity, and esophagus were contoured. With DL, contouring of the 11 OARs was < 10 s per patient. The mean DSC of seven of the 11 contoured organs ranged from 0.78 to 0.83, and the DSC values for the esophagus, brainstem, PMC and cricopharynx were 0.60, 0.64, 0.68 and 0.73, respectively[30]. The study found that for the head and neck OAR, DL-based segmentation was fast and performed well enough for treatment planning purposes for most organs and most patients.

OARs in the thorax area have also contoured for RT with AI[31-34]. Zhu *et al*[25] used CT images of 66 lung cancer cases, 30 cases for training and 36 cases for testing. CNN was used for segmentation, and compared with atlas-based automatic segmentation (ABAS). DSC, the mean surface distance (MSD), and 95% Hausdorff distance (95% HD) were used to evaluate the results. The MSD (mm) values for CNN and ABAS were 2.92 and 3.14 for the heart, 3.21 and 3.83 for the liver, 1.81 and 3.03 for ms, 2.65 and 2.67 for the esophagus, and 1.93 and 1.85 mm for the lungs. The 95% HD (mm) values for CNN and ABAS were 7.98 and 9.53 in the heart, 10.0 and 11.87 in the liver, 8.74 and 11.97 in ms, 9.25 and 9.45 in the esophagus, and 7.96 and 8.07 mm in the lungs[25]. According to the results of that study, CNN can be used in segmentation for RT of lung cancer. Zhang *et al*[33] compared CNN-based segmentation and ABAS and reported that CNN-based segmentation required 1.6 minutes per case and atlas-based contouring required 2.4 min ($P < 0.001$). Accuracy rates were measured by DSC and MSD and found that CNN-based segmentation was better than atlas-based segmentation for left lung and heart RT[33]. A study by Vu *et al*[34] that included

22411 CT images obtained from 168 cases reported training, validation, and test rates of 66%, 17% and 17%, respectively. CNN-based and atlas-based segmentation models were compared with verification by DSC and 95% HD. All differences were found to be statistically significant in favor of CNN-based segmentation[34].

Looking at other studies in the literature, Feng *et al*[32] evaluated 36 cases, with 24 used as training and 12 used as testing. The DSC obtained with 3D U-Net for medulla spinalis, right lung, left lung, heart, and esophagus were 0.89, 0.97, 0.97, 0.92, and 0.72, respectively. The corresponding MSDs were 0.66, 0.93, 0.58, 2.29 and 2.34 mm; and the 95% HDs were 1.89, 3.95, 2.10, 6.57, 8.71[32]. The conclusion was that because of the improved accuracy and low cost of OAR segmentation, DL has the potential to be clinically adopted in RT planning. Loap *et al*[31] performed AI-based heart segmentation with CT images obtained from 20 breast cancer cases. The performance of the model was evaluated by DSC, and this value was found to be 95% for the whole heart and 80% for the heart chambers[31].

Studies on OAR segmentation in the pelvic region have generally been done with cervical and prostate cancer[27,35]. The bladder, bone marrow, left femoral head, right femoral head, rectum, small intestine, and ms were contoured using CT images of 105 locally advanced cervical cancer cases. U-Net was used and the accuracy of the model was evaluated by DSC and 95% HD. The DSC of OARs ranged from 92% to 79%, with the best results in the bladder and the worst in the rectum. 95% HD values ranged between 5.09 and 1.39 mm[35]. Savenije *et al*[27] included 150 prostate cancer cases with MR imaging. DeepMedic and dense V-net were used in modeling. Bladder, rectum and femoral heads are contoured. The duration of DeepMedic, dense V-net, and atlas-based segmentation were 60 s, 4 s and 10-15 min, respectively. The accuracy of the DeepMedic algorithm that had been obtained in a feasibility study was confirmed the clinical setting in that study[27].

Additional evidence is available from a study by Ahn *et al*[36] who used CT images of 70 cases diagnosed with liver cancer, 45 for training, 15 for validation, and 19 for testing. The reference was accepted segmentation by three senior physicians. The model was created with deep CNN (DCNN). The accuracy rate was evaluated with 95% HD, DSC, volume overlap error (VOE), and relative volume difference (RVD). In ABAS, the DSCs were 0.92, 0.93, 0.86, 0.85, and 0.60 for the heart, liver, right kidney, left kidney and stomach. In the DCNN-based model, the values were 0.94, 0.93, 0.88, 0.86, and 0.73. The VOE% values in DCNN and atlas-based segmentation were 10.8 *vs* 15.17, 10.82 *vs* 13.52, 12.19 *vs* 17.51, 16.31 *vs* 25.63 and 37.53 *vs* 62.64. The RVD% values in DCNN and atlas-based segmentation were 5.17 *vs* 12.90, 1.86 *vs* 5.56, 4.53 *vs* 9.75, 2.45 *vs* 10.23 and 21.26 *vs* 50.6[36]. In that study, DL-based segmentation appeared to be more effective and efficient than atlas-based segmentation for most of the OAR in liver cancer RT.

Dolz *et al*[26] performed brainstem segmentation from the MR images of 14 brain cancer cases. A support vector machine (SVM) algorithm was used for the model, DSC, absolute volume difference (AVD) and percentage volume difference (pVD) between automatic and manual contours were used for the performance evaluation of the model. The mean values were, DSC 0.89-0.90, AVD 1.5 cm^3 and pVD 3.99%[26]. The proposed approach has consistently shown similarity to manual segmentation and can be considered promising for adoption in clinical practice. Studies that investigated segmentation of OARs are summarized in Table 1.

Learning algorithms are trained to maximize measures of similarity between outcomes and examples given to them. Therefore, although they are increasingly skilled at imitating human-drawn contours, they are limited by the quality of their training samples. Until more concrete consensus definitions are specified for boundaries, machines cannot be more accurate than the human input taken as their clinically fundamental truth. Machine "accuracy" is only considered to be meaningful in the context of individuals and institutional protocols. More case numbers and multicenter studies are needed for the development and standardization of contouring models.

Target volume contouring: Target volume contouring is a labor-intensive step in the treatment planning flow in RT. Differences in manual contouring result from variability between contours, differences in radiation oncology education, or quality differences in imaging studies. Current automatic contouring methods aim to reduce manual workload and increase contour consistency, but still tend to require significant manual editing[37]. Recent studies have shown that DL-based automatic contouring of target volumes is promising, with greater accuracy and time savings compared with atlas-based methods.

Table 1 Contouring of at-risk organs

Ref.	Tumor site	Artificial intelligence technique	Patient number	Contouring	Results
Ibragimov *et al*[28], 2017	Head-neck	CNN	50	Contoured with CT. OARs: (1) Ms; (2) Mandible; (3) Parotid; (4) SMG; (5) Larynx; (6) Pharynx; (7) Eyes; (8) Optic nerve; and (9) Optic chiasm	DSC: (1) Ms: 87%; (2) Mandible: 89.5%; (3) Right parotid gland: 77.9%; (4) Left parotid gland: 76.6%; (5) Left SMG: 69.7%; (6) Right SMG: 73%; (7) Larynx: 85.6%; (8) Pharynx: 69.3%; (9) Left eye glob: 63.9%; (10) Right eye glob: 64.5%; (11) Left optic nerve: 63.9%; (12) Right optic nerve: 64.5%; and (13) Optical chiasm: 37.4%
Chan *et al*[29], 2019	Orafarenx	LL-CNN, 2D U-Net, 3D U-Net, ST-CNN, MT-CNN	200 (160 training, 20 validation, 20 test)	Contoured with CT. OAR: (1) Mandible; (2) Right and left parotid gland; (3) Oral cavity; (4) Brain stem; (5) Larynx; (6) Esophagus; (7) Right and left SMG; and (8) Right and left TMJ	DSC (mm) for LL-CNN and RMSE: (1) Mandible: 0.91 and 0.66; (2) Right parotid gland: 0.86 and 1.67; (3) Left parotid gland: 0.85 and 1.86; (4) Oral cavity: 0.87 and 0.83; (5) Brain stem: 0.89 *vs* 0.96; (6) Larynx: 0.86 *vs* 1.34; (7) Esophagus: 0.86 *vs* 1.03; (8) Right SMG: 0.85 *vs* 1.24; (9) Left SMG: 0.84 *vs* 1.22; (10) Right TMJ: 0.87 *vs* 0.43; and (11) Left TMJ: 0.84 *vs* 0.47
Rooij *et al*[30], 2019	Head-neck	3D U-Net	157 (142 training, 15 tests)	Contoured with CT. OAR: (1) Right and left SMG; (2) Right and left parotid gland; (3) Larynx; (4) Cricopharynx,; (5) PCM; (6) UES; (7) Brain stem; (8) Oral cavity; and (9) Esophagus	DSC: (1) Right SMG: 0.81; (2) Left SMG: 0.82; (3) Right parotid gland: 0.83; (4) Left parotid gland: 0.83; (5) Larynx: 0.78; (6) Cricopharynx: 0.73; (7) PCM: 0.68; (8) UES: 0.81; (8) Brain stem: 0.64; (9) Oral cavity: 0.78; and (10) Esophagus: 0.60
Zhu *et al*[25], 2017	Lung	CNN	66 (30 training, 36 tests)	Contoured with CT. OAR: (1) Heart; (2) Liver; (3) Ms; (4) Esophagus; and (5) Lung	MSD (mm) (CNN *vs* ABAS): (1) Heart: 2.92 *vs* 3.14; (2) Liver: 3.21 *vs* 3.83; (3) Ms: 1.81 *vs* 3.03; (4) Esophagus: 2.65 *vs* 2.67; and (5) Lung: 193 *vs* 1.85; 95% HD (mm) (CNN *vs* ABAS): (1) Heart: 7.98 *vs* 9.53; (2) Liver: 10.06 *vs* 11.87; (3) Ms: 8.74 *vs* 11.97; (4) Esophagus: 9.25 *vs* 9.45; and (5) Lung: 7.96 *vs* 8.07
Zhang *et al*[33], 2020	Lung	CNN	200: training;50: validation 19: test	Contoured with CT. OAR: (1) Lungs; (2) Esophagus; (3) Heart; (4) Liver; and (5) Ms	DSC (CNN *vs* atlas based): (1) Left lung: 94.8% *vs* 93.2%; (2) Right lung: 94.3% *vs* 94.3%; (3) Heart: 89.3% *vs* 85.8%; (4) Ms: 82.1% *vs* 86.8%; (5) Liver: 93.7% *vs* 93.6%; and (6) Esophagus: 73.2% *vs* -; MSD (mm) (CNN *vs* atlas based): (1) Left lung: 1.10 *vs* 1.73; (2) Right lung: 2.23 *vs* 2.17; (3) Heart: 1.65 *vs* 3.66; (4) Ms: 0.87 *vs* 0.66; (5) Liver: 2.03 *vs* 2.11; and (6) Esophagus: 1.38 *vs* -
Vu *et al*[34], 2020	Lung	2D-CNN	168 (66% training, 17% validation, 17% testing)	Contoured with CT. OAR: (1) Ms; (2) Lungs; (3) Heart; and (4) Esophagus	DSC (CNN *vs* atlas - based model): (1) Ms: 71% *vs* 67%; (2) Right lung: 96% *vs* 94%; (3) Left lung: 96% *vs* 94%; (4) Heart: 91% *vs* 85%; and (5) Esophagus: 63% *vs* 37%; 95% HD (mm) (CNN *vs* atlas - based model): (1) Ms: 9.5 *vs* 25.3; (2) Right lung: 5.1 *vs* 8.1; (3) Left lung: 4.0 *vs* 8.0; (4) Heart: 9.8 *vs* 15.8; and (5) Esophagus: 9.2 *vs* 20
Feng *et al*[32], 2019	Lung	3D U-Net	36 (24 training, 12 tests)	Contoured with CT. OAR: (1) Ms; (2) Right lung; (3) Left lung; (4) Heart; and (5) Esophagus	DSC: (1) Ms: 0.89; (2) Right lung: 0.97; (3) Left lung: 0.97; (4) Heart: 0.92; and (5) Esophagus: 0.72; 95% HD (mm): (1) Ms: 1.89; (2) Right lung: 3.95; (3) Left lung: 2.10; (4) Heart: 6.57; and (5) Esophagus: 8.71; MSD (mm): (1) Ms: 0.66; (2) Right lung: 0.93; (3) Left lung: 0.58; (4) Heart: 2.29; and (5) Esophagus 2.34
Liu *et al*[35], 2019	Cervix	3D U-Net	105 (77 training, 14 validation, 14 tests)	Contoured with CT. OAR: (1) Bladder; (2) Bone Marrow; (3) Left femoral head; (4) Right femoral head; (5) Rectum; (6) Small intestine; and (7) Ms	DSC: (1) Bladder: 0.92; (2) Bone Marrow: 0.86; (3) Left femoral head: 0.89; (4) Right femoral head: 0.89; (5) Rectum: 0.79; (6) Small intestine: 0.83; and (7) Ms: 0.82; 95% HD (mm): (1) Bladder: 5.09; (2) Bone marrow: 1.99; (3) Left femoral head: 1.39; (4) Right femoral head: 1.43; (5) Rectum: 5.94; (6) Small intestine: 5.21; and (7) Ms: 3.26
Savenije *et al*[27], 2020	Prostate	DeepMedic and Dense V-net	48 (36 training, 16 tests) for feasibility study; 150 cases in total (97 train, 53 tests)	Contoured by MR. OAR: (1) Bladder; (2) Rectum; (3) Left femur; and (4) Right femur	DSC/95% HD (mm)/MSD (mm): (DeepMedic and dense V-net (feasibility study): (1) Bladder: 0.95/3.8/1.0; (2) Rectum: 0.85/8.3/2.1; (3) Left femur: 0.96/2.2/0.6; and (4) Right femur: 0.96/1.9/0.6; DSC/95% HD (mm)/MSD (mm): (Clinical application with DeepMedic): (1) Bladder: 0.96/2.5/0.6; (2) Rectum: 0.88/7.4/1.7; (3) Left femur: 0.97/1.6/0.5; and (4) Right femur: 0.97/1.5/0.5
Ahn *et al*[36], 2019	Liver	DCNN	70 (45 training, 15 validation, 10 tests)	Contoured with CT. OAR: (1) Heart; (2) Liver; (3) Kidney; and (4) Stomach	DSC (DCNN *vs* atlas-based contouring): (1) Heart: 0.94 *vs* 0.92; (2) Liver: 0.93 *vs* 0.93; (3) Right kidney: 0.88 *vs* 0.86; (4) Left kidney: 0.86 *vs* 0.85; and (5) Stomach: 0.73 *vs* 0.60

95% HD: 95% Hausdorff distance; ABAS: Atlas-based automatic segmentation; CNN: Convolutional neural network; CT: Computational Tomography; DCNN: Deep convolutional neural network; DSC: Dice similarity coefficient; ms: Medulla spinalis; MSD: Mean surface distance; MSD: The mean surface distance; MT-CNN: Multitask Convolutional neural network, RMSE: Root-mean-square error; OAR: Organ at risk; PCM: Pharyngeal constrictor muscle; SMG: Submandibular gland; ST-CNN: Single-task Convolutional neural network; TMJ: Temporamandibular joint; UES: Upper esophageal sphincter.

The first reason for the necessity of computer-aided delineation is the variation between contours or even between contours of the same person at different times. Chao *et al*[38] reported that differences in defining CTVs from scratch among radiation oncologists is important, and the use of computer-aided methods reduces volumetric variation and improves geometric consistency[38]. The second reason is that it is time consuming. In a study by Chao *et al*[38], computer-assisted contouring provided 36%-29% time savings for experienced physicians and 38%-47% for less experienced physicians[38]. Ikushima *et al*[39] estimated the gross tumor volume (GTV) of 14 lung cancers. Six were solid, six were part-solid, and four had mixed ground-glass opacity (GGO) using AI. Image properties around the GTV contours were taught to the SVM algorithm during training, after which the algorithm was tested to generate GTV for each voxel. Diagnostic CT, planning CT and PET were used for image properties. The final GTV contour was determined using the optimum contour selection method. DSC was used for the performance of the algorithm and was determined to be 0.77 for 14 cases. The DSC values for solid, part-solid and mixed GGO were 0.83, 0.70 and 0.76, respectively[39]. In a study conducted by Cui *et al*[40], 192 cases of lung cancer (118 solid, 53 part-solid, and 21 pure GGO) with stereotactic body radiotherapy (SBRT) were contoured with dense V-networks using planning it. Of those, 147 cases were for training, 26 for validation, and 19 cases were for testing. Evaluation was performed with a DSC and HD 10-fold cross validation test. The 3D-DSC values were 0.838 ± 0.074, 0.822 ± 0.078, and 0.819 ± 0.059 for solid, part-solid, and GGO tumors respectively. The HD value of each inner group was 4.57 ± 2.44 mm[40]. The proposed approach has the potential to assist radiation oncologists in identifying GTVs for planning treatment of lung cancer SBRT.

Zhong *et al*[41] performed segmentation with 3-D DL and fully convolutional networks (DFCN) using both PET and BT images of 60 lung SBRT cases. Delineation was performed by three senior physicians. A simultaneous truth and performance level estimation algorithm was accepted as a reference, and DSC was used to evaluate DFCN performance. The mean DSCs were for 0.861 ± 0.037 for CT and 0.828 ± 0.087 for PET[41]. Kawata *et al*[42] used pixel-based MÖ techniques such as fuzzy-c-means clustering (FCM), artificial neural network (ANN), and SVM to evaluate the GVT of 16 lung cancer tumors (six solid, four GGO, six part-solid) for SBRT by AI using PET/CT. The performance of the algorithms was determined by DSC. The DSC values for FCM, ANN, and SVM were 0.79 ± 0.06, 0.76 ± 0.14 and 0.73 ± 0.14, respectively[42]. FCM had the highest accuracy rates of GTV contouring compared with the other algorithms.

There are also GTV and CTV contouring studies with AI in head and neck cancers[43-47]. In a study by Li *et al*[43], tumor segmentation was performed in nasopharyngeal cancer by using CT images. The U-Net model was used, 302 cases

were used for training, 100 for validation, and 100 for testing. In the U-Net model, DSC was found to be 65.8% for lymph nodes and 74.0% for tumor segmentation. Automatic delineation was calculated as 2.6 h per patient and manual delineation as 3 h[43]. This study found that DL increased the accuracy, consistency, and efficiency of tumor delineation and that additional physician input might be required for lymph node delineation. Multimodality medical images can be very useful for automated tumor segmentation as they provide complementary information that can make the segmentation of tumors more accurate. Ma *et al*[44] used multimodality CNN (M-CNN) based methods to investigate the segmentation of nasopharyngeal cancer using CT and MR images. M-CNN is designed to co-learn the segmentation of matched CT-MR images. Considering that each modality has certain distinctive features, it was planned to create a combined-CNN (C-CNN) using single-modality (S-CNN) and higher-layer features derived from M-CNN. Ninety CT and MR images were used, and positive predictive value (PPV), sensitivity (SE), DSC, and average symmetric surface distance (ASSD) were used to evaluate modalities. The PPV, SE, DSC and ASSD obtained by C-CNN, were 0.797 ± 0.109, 0.718 ± 0.121, 0.752 ± 0.043, and 1.062 ± 0.298 mm respectively. The included two main models, M-CNN and C-CNN, which can integrate complementary information from CT and MR images for tumor identification. The results in the clinical CT-MR dataset show that the proposed M-CNN can learn the correlations of two modalities and tumor segmentation together and perform better than using a single modality[44].

Zhao *et al*[45] used PET-CT and FCN to contour 30 nasopharyngeal cancer tumors. The mean DSC was 87.47% after threefold cross validation. Guo *et al*[46] performed GTV contouring with Dense Net and 3D U-Net using PET/CT and PET-CT in 250 head and neck cancer patients. DSC, MSD, and HD95 were calculated for each of the three imaging methods separately. For Dense Net, the DSC values were 0.73 for PET-CT, 0.67 for PET, and 0.32 for CT. The DSC for 3D-U-Net and PET-CT was 0.71. MSD, HD for Dense Net PET-BT were 2.88, 6.48 and 3.96 mm, respectively. For Dense Net PET, the MSD, and HD95 DC were 3.38, 8.29 and 5.56 mm, respectively. For 3D U-Net, the MSD, HD95, DC were 2.98, 7.57 and 4.40 mm respectively[46]. In a study using a deep deconvolutional neural network (DDNN), the GTV_{tumor}, $GTV_{lymph\ node,}$ and CTV were determined from CT images of 230 nasopharyngeal cancer cases that were randomly allocated to 184 cases for training and 46 cases for testing. The DSC values were 80.9% for GTV_{tumor}, 62.3% for $GTV_{lymph\ node}$, and 82.6% for CTV[47].

AI-based contouring studies have also been performed in primary brain tumors and brain metastases[48-53]. In a study by Jeong *et al*[51], T1-weighted dynamic contrast-enhanced (DCE) perfusion MR images of 21 patients diagnosed with brain tumors were used for tumor segmentation. 3D mask region-based CNN (R-CNN) was used and algorithm performance was evaluated with DSC, HD, MSD, and center of mass distance. The values were 0.90 ± 0.04, 7.16 ± 5.78 mm, 0.45 ± 0.34 mm and 0.86 ± 0.91 mm, respectively[51]. The results support the feasibility of accurate localization and segmentation of brain tumors from DCE perfusion MRIs. Segmentation with 3D mask R-CNN in DCE perfusion imaging holds promise for future clinical use. Tang *et al*[53] described postoperative glioma segmentation of the CTV region using MR image information on CT. A deep feature fusion model (DFFM) guided by multisequence MR was used in CT images for postop glioma segmentation. DFFM is a multisequence MR-guided CNN that simultaneously learns deep features from CT and multisequence MR images and then combines the two deep features. In this study, 59 BT and MR (T1/T2-weighted FLAIR, T1-weighted contrast-enhanced, T2-weighted) data sets were used. The DSCs were 0.836 and 0.836[51]. Given the DSC rate, this algorithm can be used in the presegmentation stage to reduce the workload of the radiation oncologist.

Liver tumor segmentation with CT is difficult because the image contrast between liver tumors and healthy tissues is low, the boundary is blurred, and images of the liver tumor are complex, and vary in size, shape, and location. To solve these problems, Meng *et al*[54] performed liver tumor segmentation with 3D dual-path multiscale CNN (TDP-CNN). In the study, 81 CT images were used for training and 25 were used for the test. Tumor segmentation determined by an experienced radiologist was used as a reference. Performance evaluation was determined as DSC, HD average distance, and the values were 0.689, 7.69, and 1.07mm[54].

There are also studies using AI in pelvic tumor and CTV contouring[55-59]. In a prostate cancer study, MR images and the DeepLabV3 + method were used for with target volume segmentation. Volumetric DSC and surface DSC were used to evaluate performance, and these values were 0.83 ± 0.06 and 0.85 ± 0.11, respectively[56]. According to this model, the planning workflow can be accelerated with MR. Voxel-based ML was evaluated, and MR images of 78 cases were used in a study of tumor

delineation in locally advanced cervical cancer. The model was trained according to the delineation of two radiologists, mean sensitivity was 94% and specificity was 52%[57]. CT images were used for CTV delineation in rectal cancer, and 218 randomly selected cases were used for training and 60 cases for validation. Deep dilated CNN (DDCNN) was used and the DSC for the model was 87.7%[59]. According to that study, the accuracy rate was high and effective in CTV segmentation in the DDCNN rectal cancer. Deep dilated residual network (DD-ResNet) was used in breast cancer CTV contouring, and the model was compared with DDCNN and DDNN. CT images of 800 breast cancer cases were used in the study, and the training/test rate was determined as 80%/20%. Mean DSC was used for segmentation accuracy. For the right and left breast, DD-ResNet was 0.91 and 0.91, 0.85 and 0.85, 0.88 and 0.87 for DDCNN and DDNN, respectively. HD values were 10.5 and 10.7 mm, 15.1 and 15.6 mm, and 13.5 and 14.1 mm, respectively. Mean segmentation times were 4, 21 and 15 s per patient[60]. The method proposed in the study contoured the CTV in a short time and with high accuracy. The studies of target volume segmentation are summarized in Table 2. More cases and multidisciplinary studies are needed to reduce the heterogeneity in tumor response and in GTV and CTV contouring, shorten the contouring step, and create standard delineations.

RADIOTHERAPY PLANNING

RT planning process is quite complex. A mistake during planning can lead to life-threatening situations such as tumor incontinence or high doses of radiation to normal tissue. As technology advances, the margin given to the tumor also decreases, so even with a small margin of error, it is possible to miss the tumor geographically. After target volumes and OARs are defined, the planning process continues with the determination of dosimetric targets for targets and OARs, selection of an appropriate treatment technique [*e.g.*, 3DCRT, intensity-adjusted RT (IMRT), volumetric modulated arc therapy (VMAT), protons], the achievement of planning goals, and evaluation and approval of the plan. Treatment planning, which is an RT design for each case, can be considered as both a science and an art.

Because of the complex mathematics and physics involved, RT planning includes computer-aided systems. During planning, humans interact many times with the computer-aided system, using their experience and skills to ensure the satisfactory quality of each plan. Planning is a very complex process. There are AI studies related to the planning steps of RT, such as dose calculation, dose distribution, dose-volume histogram (DVH), patient-specific dose calculation, IMRT area determination, beam angle determination, real-time tumor tracking, and replanning in adaptive RT[61-71].

The purpose of researching the dose calculation algorithm is to increase calculation accuracy while maximizing computational efficiency. In the study conducted by Zhu *et al*[61], it was aimed to calculate the 3D distribution of total energy release per unit mass and electron density based on CNN. Twelve sets of CT images were used for training, and a random beam configuration was created with a convolution/superposition (CCCS) algorithm. 7500 samples were created for each single-energy photon model training set and 1500 samples for validation. Training included 0.5 MeV, 1 MeV, 2 MeV, 3 MeV, 4 MeV, 5 MeV, and 6 MeV monoenergetic photon models. To evaluate its usability under linear accelerator (Linac) conditions, 12 additional new CT images with different anatomical regions and 1512 samples were used for testing. For all anatomies, the mean value for the criterion of 3%/2mm, 95% lower confidence limit, and 95% upper confidence limit were 99.56%, 99.51%, and 99.61%, respectively. In that study, DL was investigated for CCCS dose calculation[61]. With DL, calculation accuracy can be improved and calculation efficiency can be increased, and the method can speed up dosing algorithms and also has great potential in adaptive RT.

In their study, Zhang *et al*[62] aimed to estimate voxel level doses by integrating the distance information between the planning target volume (PTV) and OAR as well as the image information into the DCNN. First, they created a four-channel feature map consisting of PTV image, OAR image, CT image, and distance image. A neural network was created and trained for dose estimation at the voxel level. Given that the shape and size of OARs are highly variable, dilated convolution was used to capture features from multiple scales. The network was evaluated by five-fold cross validation based on 98 clinically validated treatment plans. The voxel level mean absolute error values of the DCNN for PTV, left lung, right lung, heart, spinal cord and body were 2.1%, 4.6%, 4.0%, 5.1%, 6.0% and 3.4% respectively[62]. This method significantly improved the accuracy of the dose distribution estimated by the DCNN model. In their

Table 2 Target volume segmentation

Ref.	Tumor site	Artificial intelligence technique	Patient number	Contouring	Results
Ikushima *et al*[39], 2017	Lung	SVM	14 (solid: 6, GGO: 4, mixed GGO: 4)	GTV	DSC: (1) 0.777 for 14 cases; and (2) 0.763 for GGO, 0.701 for mixed GGO
Cui *et al*[40], 2021	Lung	DVNs	192 (solid: 118, part-solid:53, pure GGO: 21)	GTV	3D-DSC: (1) Solid: 0.838 ± 0.074; (2) Part-solid: 0.822 ± 0.078; and (3) GGO: 0.819 ± 0.059
Zhong *et al*[41], 2019	Lung	3D-DFCN	60	GTV	DSC: (1) CT: 0.861 ± 0.037; and (2) PET: 0.828 ± 0.087
Kawata *et al*[42], 2017	Lung	FCM, ANN, SVM	16 (solid: 6, GGO:4, part-solid GGO:6)	GTV	DSC: (1) FCM-based framework:0.79 ± 0.06; (2) ANN-based framework: 0.76 ± 0.14; and (3) SVM-based framework: 0.73 ± 0.14
Li *et al*[43], 2019	Nasopharynx	U-Net	502	GTV	DSC: (1) Lymph nodes: 65.86%; (2) Primary tumor: 74.00%; HDs: (1) Lymph nodes: 32.10 mm; and (2) Primary tumor:12.85 mm
Zhao *et al*[45], 2019	Nasopharynx	FCN	30	GTV	DSC: 87.47%
Guo *et al*[46], 2020	Head and neck	Dense Net and 3D U-Net	250	GTV	DSC: (1) Dense Net with PET/CT: 0.73; (2) Dense Net with PET: 0.67; (3) Dense Net with CT: 0.32; and (4) 3D U-Net with PET/CT: 0.71; MSD: (1) Dense Net with PET/CT: 2.88; (2) Dense Net with PET: 3.38; (3) Dense Net with CT: -; and (4) 3D U-Net with PET/CT: 2.98; HD_{95}: (1) Dense Net with PET/CT: 6.48; (2) Dense Net with PET: 8.29; (3) Dense Net with CT: -; and (4) 3D U-Net with PET/CT: 7.57
Jeong *et al*[51], 2020	Brain	3D-R-CNN	21	GTV	DSC: 0.90 ± 0.04; HD: 7.16 ± 5.78 mm; MSD: 0.45 ± 0.34 mm; Center of mass distance: 0.86 ± 0.91 mm
Meng *et al*[54], 2020	Liver	TDP-CNN	106	GTV	DSC: 0.689; HD: 7.69mm; Average distance: 1.07 mm
Elguindi *et al*[56], 2019	Prostate	2D-CNN, DeepLabV3 +	50	Prostate	Volumetric DSCL: 0.83 ± 0.06; Surface DSC: 0.85 ± 0.11
Men *et al*[59], 2017	Rectum	DDCNN	278	CTV	DSC: 87.7%

ANN: Artificial neural network; CT: Computed tomography; CTV: Clinical target volume.; DDCNN: Deep dilated convolutional neural network; DFCN: Fully convolutional network; DSC: Dice similarity coefficient; DVNs: Dense V-network; FCM: Fuzzy-c-means clustering method; GGO: Ground-glass opacity; GTV: Gross tumor volume; HD: Hausdorff distance; MSD: Mean surface distance; PET: Positron emission tomography; R-CNN: Region-based convolutional neural network; SVM: Support vector Machine; SVM: Support vector machine; TDP-CNN: Three-dimensional dual-path multiscale convolutional neural network.

studies, Fan *et al*[64] aimed to develop a 3D dose estimation algorithm based on DL and create a treatment plan based on the dose distribution for IMRT. The DL model was trained to estimate a dose distribution based on patient-specific geometry and prescription dose. A total of 270 head and neck cancer cases, 195 in the training data set, 25 in the validation set, and 50 in the test set, were included in the study. All cases were treated with IMRT. The model input consisted of CT images and contours that

defined the OAR and plot target volumes. The algorithm output was trained to estimate the dose distribution from the CT image slice. The resulting estimation model was used to estimate the patient dose distribution. An optimization target function was then created based on the estimated dose distributions for automatic plan generation. In the study, Differences between the prediction and the actual clinical plan in DVH for all OARs were not significant except for the brainstem, right, and left lens. Differences between PTVs ($PTV_{70.4}$, PTV_{66}, $PTV_{60.8}$, PTV_{60}, PTV_{56}, PTV_{54}, PTV_{51}) in the estimated and the actual plan were significant only for $PTV_{70.4}$[64]. In that study, optimization based on 3D dose distribution and an automatic RT planning system based on 3D dose estimation were developed. The model is a promising approach to realize automatic treatment planning in the future.

Ma *et al*[65] created a DVH prediction model that depended on support vector regression as the backbone of the ML model. A database containing VMAT plans of 63 prostate cancer cases was used, and a PTV plan was created for each patient. A correlative relationship between the OAR DVH (model input) of the PTV plan and the corresponding DVH (model output) of the clinical treatment plan was established with 53 training cases. The predictive model was tested with a validation group of ten cases. In the control of dosimetric endpoints for the training group, 52 of 53 bladder cases (98%) and 45 of 53 rectum cases were found to be within a 10% error limit. In the validation test group, 92% of the bladder cases and 96% of the rectum cases were within the 10% error limit. Eight of the ten validation plans (80%) were found to be within the 10% error margin for both rectum and bladder[65]. In that study, only the PTV plan was used for DVH estimation and an ML model was created based on new dosimetric characteristics. The framework had high accuracy for predicting the DVH for VMAT plans.

In lung cancer, as in other types of cancer, optimum selection of radiation beam directions is required to ensure effective coverage of the target volume by external RT and to prevent unnecessary doses to normal healthy tissues. IMRT planning is a lengthy process that requires the planner to iterate between selecting beam angles, setting dose-volume targets, and conducting IMRT optimization. The beam angle selection is made according to the planner's clinical experience. Mahdavi *et al*[67] planned to create a framework that used ML to automatically select treatment beam angles in thoracic cancers, intended to increase computational efficiency. They created an automatic beam selection model based on learning the relationship between beam angles and anatomical features. The plans of 149 cases who underwent clinically approved thoracic IMRT were used in the study. Twenty-seven cases were randomly selected and used to test the automated plan and the clinical plan. When the estimated and clinically used beam angles were compared, a good mean agreement was observed between the two (angular distance 16.8 ± 10◦, correlation 0.75 ± 0.2). The target volume of automated and clinical plans was found to be equivalent when evaluated in terms of winding and the OAR. The vast majority of plans (93%) were approved as clinically acceptable by three radiation oncologists[69].

Treatment planning is an important step in the RT workflow. It has become more sophisticated in the past few decades with the help of computer science, allowing planners to design highly complex RT plans to minimize damage of normal tissue while maintaining adequate tumor control. A need of individual patient plans has resulted in treatment planning becoming more labor-intensive and time consuming. Many algorithms have been developed to support those involved in RT planning. The algorithms have had a major impact on focusing on automating and/or optimizing the planning process and improving treatment planning efficiency and quality. Studies of treatment planning are summarized in Table 3.

QUALITY ASSURANCE

Quality assurance (QA) is crucial in order to evaluate the RT plan and detect and report errors. Features of RT QA programs such as error detection, and prevention, and treatment device QA are very suitable for AI application[72-75]. Li *et al*[73] developed an application to estimate the performance of medical linear accelerators (Linacs) over time. Daily QA of RT in cancer treatment closely monitors Linac performance and is critical for the continuous improvement of patient safety and quality of care. Cumulative QA measures are valuable for understanding Linac behavior and enabling medical physicists to detect disturbances in output and take preventive action. Li *et al*[73] used a time series estimation model of ANNs and an autoregressive moving average to analyze 5-yr Linac QA data. Verification tests and

Table 3 Radiotherapy planning

Ref.	Aim	Patient number	Artificial intelligence technique	Results
Zhu *et al*[61], 2020	Calculating TERMA and ED	24	CNN	3%/2 mm, 95% LCL, and 95% UCL to 99.56%, 99.51%, 99.61%
Zhang *et al*[62], 2020	Making voxel level dose estimation by integrating the distance information between PTV and OAR	98	DCNN	MAEV: (1) PTV: 2.1%; (2) Left lung: 4.6%; (3) Right lung: 4.0%; (4) Heart: 5.1%; (5) Spinal cord: 6.0%; and (6) Body: 3.4%
Fan *et al*[64], 2019	Developing a 3D dose estimation algorithm	270		Significant difference was found between the estimated and the actual plan in only $PTV_{70.4}$
Ma *et al*[65], 2019	Creating a DVH prediction model	63	SVR	The error limit of 10% for the bladder and rectum was 92% and 96%
Mahdavi *et al*[69], 2015	Selecting treatment beam angles in thoracic cancers	149	ANN	The majority of plans (93%) were approved as clinically acceptable by three radiation oncologists

ANN: Artificial neural networks.; CNN: Convolutional neural network; DCNN: Deep convolutional neural network; DVH: Dose value histogram; ED: Electron density; LCL: Lower confidence limit; MAEV: Voxel level mean absolute error; OAR: Organ at risk; PTV: Planning target volume; SVR: Support vector regression; TERMA: Three-dimensional distribution of total energy release per unit mass; UCL: Upper confidence limit.

other evaluations were made for all models and they reported that the ANN algorithm can be applied correctly and effectively in dosimetry and QA[73]. Valdes *et al*[72] developed AI applications to predict IMRT QA transition rates and automatically detect problems in the Linac imaging system. Carlson *et al*[76] developed an ML approach to predict multileaf collimator (MLC) position errors. Inconsistencies between planned and transmitted motions of multileaf collimators are a major source of error in dose distribution during RT. In their study, factors such as leaf movement parameters, leaf position and speed, leaf movement towards or away from the isocenter of the MLC were calculated from plan files of AI forecasting models. Position differences between synchronized DICOM-RT planning files and DynaLog files reported during QA delivery were used for training the models. To assess the effect on the patient, the DVH in the treated positions and the planned and anticipated DVHs were compared. In all cases, they found that the DVH parameters predicted for the OAR, especially around the treatment area, were closer to the DVHs in the treated position than to the planned DVH parameters[76].

The use of treatment plan features to predict patient-specific QA measurement results facilitate development of automated pretreatment validation workflows or provide a virtual assessment of treatment quality. Granville *et al*[77] trained a linear support vector classifier to classify the results of patient-specific VMAT QA measurements, using the complexity of the treatment plan and characteristics that define the Linac performance criteria. The "targets" in this model are simple classifications that represent the median dose difference between measured and expected dose distributions; median dose deviation was considered "hot" if > 1%, "cold" if < 1%, and "normal" if ± 1%. A total of 1620 patient-specific QA measurements were used for model development and testing' and 75% of the data was used for model development and validation. The remaining 25% was used for the independent evaluation of model performance. Receiver operating characteristic (ROC) curve analysis was used to evaluate model performance. Of the ten variables that are considered important for prediction, half consist of treatment plan characteristics, and half are QA measures that characterize Linac performance. For this model, the micro-averaged area under the ROC curve was 0.93, and the macro-averaged area under the ROC curve was 0.88[77]. The study demonstrates the potential of using both treatment plan features and routine Linac QA results in the development of ML models for patient-specific VMAT QA measurements.

RT APPLICATION, SETUP

During radiation therapy, treatment may need to be adjusted to ensure that the plan is properly implemented. Need of adjustment may result from both online factors such as the patient's pretreatment position, and longer-term factors related to anatomical

changes and response to treatment. Images taken before treatment should be aligned with the images in the planning CT and kept in alignment. Although many modern Linac devices currently have daily "cone-beam" CT (CBCT) using mega-voltage X-rays for treatment confirmation, but that imaging is not sufficient to distinguish soft tissue structures. However, those images are considered suitable for image-guided RT as they are used to adapt the treatment plans to the daily anatomy of the patient and to reduce intra-fractional shifts. When performing daily RT, the CBCT should be reviewed before each treatment. Two, or at least one experienced RT technician, are required for this procedure. When the RT technician sees an anatomical difference between the CBCT and the planning CT, she/he should inform the radiation oncologist and medical physicist. At that stage, it is necessary to decide whether to continue treatment with the difference or to require a new CBCT. Each of the steps delays patient treatment and causes a significant increase in the RT department workload. All this opens a path for the growth of AI in parallel with the training program in radiation oncology. In addition to the ability of existing staff to cope with the growing workload, innovations in modern technology and the ability to benefit from it are limited by access to adequate human resources[78]. In addition, AI replanning has been used to identify candidates for adaptive RT. Based on anatomical and dosimetric variations such as shrinkage of the tumor, weakening of the patient, or edema, classifiers and clustering algorithms have been developed to predict the patients who will benefit most from updated plans during fractionated RT[71,79]. However, it should also be kept in mind that the algorithm will mimic past protocols rather than determine the ideal time for replanning because AI learns from data about previous patients, their plans, and adaptive RT.

PATIENT FOLLOW-UP

AI has the potential to change the way radiation oncologists follow definitive-treated patients. After surgery, the tumor may disappear during imaging, and tumor markers can quickly normalize. In contrast, imaging changes such as loss of contrast-enhancement, PET involvements or diffusion restriction, or size reduction, and the response of tumor markers after RT are gradual. Those characteristics are monitored regularly over time, and response assessments are made according to changes that are complemented by clinical experience and are considered indicative of therapeutic efficacy. Time is required for this assessment. However, if cases that will not respond to treatment can be predicted earlier, additional doses of RT or additional systemic treatments may be introduced earlier, which may improve oncological outcomes. In this context, early work in the field of radiology is promising. In radiology, quantitative features are extracted based on size and shape, image density, texture, relationships between voxels, and some characteristics to typify an image. AI algorithms can be used to correlate image-based features with biological observations or clinical outcomes[80-85]. The use of AI techniques for response and survival prediction in RT patients is a serious opportunity to further improve decision support systems and provide an objective assessment of the relative benefits of various treatment options for patients.

Cancer is the most common cause of death in developed countries, and it is estimated that the number of cases will increase further in aging populations[86,87]. Therefore, cancer research will continue to be the top priority for saving lives in the next decade. Prognosis studies have been conducted with AI on many types of cancer. The use of AI techniques for response and survival prediction in RT patients is a serious opportunity to further improve decision support systems and provide an objective assessment of the relative benefits of various treatment options for patients.

Six different ML algorithms were evaluated in a prognosis study with 72 cases of nasopharyngeal cancer. Age, weight loss, initial neutrophil/lymphocyte ratio, initial lactate dehydrogenase and hemoglobin values, RT time, tumor size, concurrent CT number, and T and N stage were determined as critical variables. The highest performing model among logistic regression, ANN, XGBoost, support-vector clustering, random forest, and Gaussian Naïve Bayes algorithms was determined as Gaussian Naïve Bayes, and the accuracy rate was found to be 88% (CI: 0.68-1)[88]. In a study using radionics obtained from clinical and PET-CT, prognosis was evaluated in 101 lung cancer cases, with 67% used for training and 33% validation and testing. The highest accuracy rate was achieved with an SVM algorithm that had an accuracy rate of 84%, a sensitivity of 86%, and a specificity of 82%[89]. In another study in which prognosis was predicted in prostate cancer, somatic gene mutations were evaluated

and an accuracy rate of 66% was obtained with an SVM algorithm[90]. Post cystectomy bladder cancer prognosis was evaluated in 3503 cases using an SVM algorithm. Recurrence, 1-, 3, and 5-yr survival rates were estimated with sensitivity and specificity above 70%[91]. In a study including 75 gastric cancer patients, the accuracy of survival, distant metastasis, and peritoneal metastasis predictions were 81% for GNB, 86% for XGBoost, and 97% for Random Forest (97%)[92]. Pham *et al*[93] used AI to detect DNp73 expression associated with 5-yr overall survival and prognosis in 143 rectal cancer cases. Ten different CNN algorithms were used, and each immunochemical image was resized. For the algorithm, 90% of the images were used in training and 10% as test data. The accuracy of ten algorithms varied between 90% and 96%[93].

In oncological treatment, forecasting is crucial in the decision-making process because survival prediction is critical in making palliative *vs* curative treatment decisions. In addition, the estimation of remaining life expectancy can be an incentive for patients to live a fuller or more fulfilling life. It is also a question of which answer is sought by health insurance companies. Survival statistics assist oncologists in making treatment decisions. However, these are data from large and heterogeneous groups and are not well suited to predict what will happen to a specific patient. AI algorithms for the prediction of RT and chemotherapy oncological outcomes have attracted considerable attention recently. In cases diagnosed with cancer, predicting survival is critical for improving treatment and providing information to patients and clinicians. Considering the data set of rectal cancer patients with specific demographic, tumor, and treatment information, it is a crucial issue whether patient survival or recurrence can be predicted by any parameter. Today, many hospitals store medical records as digital data. By evaluating these large data sets using AI techniques, it may be possible to predict patient treatment outcomes, plan individualized patient treatment, improve corporate performance, and regulate health insurance premiums.

CONCLUSION

Although AI can take place at every step in radiation oncology, from patient consultation to patient monitoring, and can contribute to the clinician and the society, there are still many challenges and problems to be solved. Initially, Large data sets should be created for AI and then undergo continuing improvement. The development of estimation tools with a wide variety of variables and models limits the comparability of existing studies and the use of standards. Estimation algorithms can be standardized by sharing data between centers, data diversity, and establishing immense databases. In addition, models can be made clinically applicable by updating with entry of new data into the models. Today, the accuracy and quality of data are also of great importance, as no AI algorithm can fix problems in training data.

REFERENCES

1 **Meyer P**, Noblet V, Mazzara C, Lallement A. Survey on deep learning for radiotherapy. *Comput Biol Med* 2018; **98**: 126-146 [PMID: 29787940 DOI: 10.1016/j.compbiomed.2018.05.018]

2 **LeCun Y**, Bengio Y, Hinton G. Deep learning. *Nature* 2015; **521**: 436-444 [PMID: 26017442 DOI: 10.1038/nature14539]

3 **Jarrett D**, Stride E, Vallis K, Gooding MJ. Applications and limitations of machine learning in radiation oncology. *Br J Radiol* 2019; **92**: 20190001 [PMID: 31112393 DOI: 10.1259/bjr.20190001]

4 **Boldrini L**, Bibault JE, Masciocchi C, Shen Y, Bittner MI. Deep Learning: A Review for the Radiation Oncologist. *Front Oncol* 2019; **9**: 977 [PMID: 31632910 DOI: 10.3389/fonc.2019.00977]

5 **Chen C**, He M, Zhu Y, Shi L, Wang X. Five critical elements to ensure the precision medicine. *Cancer Metastasis Rev* 2015; **34**: 313-318 [PMID: 25920354 DOI: 10.1007/s10555-015-9555-3]

6 **Bibault JE**, Giraud P, Burgun A. Big Data and machine learning in radiation oncology: State of the art and future prospects. *Cancer Lett* 2016; **382**: 110-117 [PMID: 27241666 DOI: 10.1016/j.canlet.2016.05.033]

7 **Huynh E**, Hosny A, Guthier C, Bitterman DS, Petit SF, Haas-Kogan DA, Kann B, Aerts HJWL, Mak RH. Artificial intelligence in radiation oncology. *Nat Rev Clin Oncol* 2020; **17**: 771-781 [PMID: 32843739 DOI: 10.1038/s41571-020-0417-8]

8 **Oberije C**, De Ruysscher D, Houben R, van de Heuvel M, Uyterlinde W, Deasy JO, Belderbos J, Dingemans AM, Rimner A, Din S, Lambin P. A Validated Prediction Model for Overall Survival From Stage III Non-Small Cell Lung Cancer: Toward Survival Prediction for Individual Patients. *Int J Radiat Oncol Biol Phys* 2015; **92**: 935-944 [PMID: 25936599 DOI: 10.1016/j.ijrobp.2015.02.048]

9 **Sinsky C**, Colligan L, Li L, Prgomet M, Reynolds S, Goeders L, Westbrook J, Tutty M, Blike G.

Allocation of Physician Time in Ambulatory Practice: A Time and Motion Study in 4 Specialties. *Ann Intern Med* 2016; **165**: 753-760 [PMID: 27595430 DOI: 10.7326/M16-0961]

10 **Lin SY**, Shanafelt TD, Asch SM. Reimagining Clinical Documentation With Artificial Intelligence. *Mayo Clin Proc* 2018; **93**: 563-565 [PMID: 29631808 DOI: 10.1016/j.mayocp.2018.02.016]

11 **Luh JY**, Thompson RF, Lin S. Clinical Documentation and Patient Care Using Artificial Intelligence in Radiation Oncology. *J Am Coll Radiol* 2019; **16**: 1343-1346 [PMID: 31238022 DOI: 10.1016/j.jacr.2019.05.044]

12 **Feng M**, Valdes G, Dixit N, Solberg TD. Machine Learning in Radiation Oncology: Opportunities, Requirements, and Needs. *Front Oncol* 2018; **8**: 110 [PMID: 29719815 DOI: 10.3389/fonc.2018.00110]

13 **Xiang L**, Wang Q, Nie D, Zhang L, Jin X, Qiao Y, Shen D. Deep embedding convolutional neural network for synthesizing CT image from T1-Weighted MR image. *Med Image Anal* 2018; **47**: 31-44 [PMID: 29674235 DOI: 10.1016/j.media.2018.03.011]

14 **Adrian G**, Konradsson E, Lempart M, Bäck S, Ceberg C, Petersson K. The FLASH effect depends on oxygen concentration. *Br J Radiol* 2020; **93**: 20190702 [PMID: 31825653 DOI: 10.1259/bjr.20190702]

15 **Maxim PG**, Tantawi SG, Loo BW Jr. PHASER: A platform for clinical translation of FLASH cancer radiotherapy. *Radiother Oncol* 2019; **139**: 28-33 [PMID: 31178058 DOI: 10.1016/j.radonc.2019.05.005]

16 **Vozenin MC**, De Fornel P, Petersson K, Favaudon V, Jaccard M, Germond JF, Petit B, Burki M, Ferrand G, Patin D, Bouchaab H, Ozsahin M, Bochud F, Bailat C, Devauchelle P, Bourhis J. The Advantage of FLASH Radiotherapy Confirmed in Mini-pig and Cat-cancer Patients. *Clin Cancer Res* 2019; **25**: 35-42 [PMID: 29875213 DOI: 10.1158/1078-0432.CCR-17-3375]

17 **Sheng K**. Artificial intelligence in radiotherapy: a technological review. *Front Med* 2020; **14**: 431-449 [PMID: 32728877 DOI: 10.1007/s11684-020-0761-1]

18 **Viergever MA**, Maintz JBA, Klein S, Murphy K, Staring M, Pluim JPW. A survey of medical image registration - under review. *Med Image Anal* 2016; **33**: 140-144 [PMID: 27427472 DOI: 10.1016/j.media.2016.06.030]

19 **Wu G**, Kim M, Wang Q, Munsell BC, Shen D. Scalable High-Performance Image Registration Framework by Unsupervised Deep Feature Representations Learning. *IEEE Trans Biomed Eng* 2016; **63**: 1505-1516 [PMID: 26552069 DOI: 10.1109/TBME.2015.2496253]

20 **Roques TW**. Patient selection and radiotherapy volume definition - can we improve the weakest links in the treatment chain? *Clin Oncol (R Coll Radiol)* 2014; **26**: 353-355 [PMID: 24667211 DOI: 10.1016/j.clon.2014.02.013]

21 **Weiss E**, Hess CF. The impact of gross tumor volume (GTV) and clinical target volume (CTV) definition on the total accuracy in radiotherapy theoretical aspects and practical experiences. *Strahlenther Onkol* 2003; **179**: 21-30 [PMID: 12540981 DOI: 10.1007/s00066-003-0976-5]

22 **Sharp G**, Fritscher KD, Pekar V, Peroni M, Shusharina N, Veeraraghavan H, Yang J. Vision 20/20: perspectives on automated image segmentation for radiotherapy. *Med Phys* 2014; **41**: 050902 [PMID: 24784366 DOI: 10.1118/1.4871620]

23 **Peressutti D**, Schipaanboord B, van Soest J, Lustberg T, van Elmpt W, Kadir T, Dekker A, Gooding M. TU-AB-202-10: how effective are current atlas selection methods for atlas-based Auto-Contouring in radiotherapy planning? *Medical Physics* 2016; **43**: 3738-3739 [DOI: 10.1118/1.4957432]

24 **Liang S**, Tang F, Huang X, Yang K, Zhong T, Hu R, Liu S, Yuan X, Zhang Y. Deep-learning-based detection and segmentation of organs at risk in nasopharyngeal carcinoma computed tomographic images for radiotherapy planning. *Eur Radiol* 2019; **29**: 1961-1967 [PMID: 30302589 DOI: 10.1007/s00330-018-5748-9]

25 **Zhu J**, Zhang J, Qiu B, Liu Y, Liu X, Chen L. Comparison of the automatic segmentation of multiple organs at risk in CT images of lung cancer between deep convolutional neural network-based and atlas-based techniques. *Acta Oncol* 2019; **58**: 257-264 [PMID: 30398090 DOI: 10.1080/0284186X.2018.1529421]

26 **Dolz J**, Laprie A, Ken S, Leroy HA, Reyns N, Massoptier L, Vermandel M. Supervised machine learning-based classification scheme to segment the brainstem on MRI in multicenter brain tumor treatment context. *Int J Comput Assist Radiol Surg* 2016; **11**: 43-51 [PMID: 26206715 DOI: 10.1007/s11548-015-1266-2]

27 **Savenije MHF**, Maspero M, Sikkes GG, van der Voort van Zyp JRN, T J Kotte AN, Bol GH, T van den Berg CA. Clinical implementation of MRI-based organs-at-risk auto-segmentation with convolutional networks for prostate radiotherapy. *Radiat Oncol* 2020; **15**: 104 [PMID: 32393280 DOI: 10.1186/s13014-020-01528-0]

28 **Ibragimov B**, Xing L. Segmentation of organs-at-risks in head and neck CT images using convolutional neural networks. *Med Phys* 2017; **44**: 547-557 [PMID: 28205307 DOI: 10.1002/mp.12045]

29 **Chan JW**, Kearney V, Haaf S, Wu S, Bogdanov M, Reddick M, Dixit N, Sudhyadhom A, Chen J, Yom SS, Solberg TD. A convolutional neural network algorithm for automatic segmentation of head and neck organs at risk using deep lifelong learning. *Med Phys* 2019; **46**: 2204-2213 [PMID: 30887523 DOI: 10.1002/mp.13495]

30 **van Rooij W**, Dahele M, Ribeiro Brandao H, Delaney AR, Slotman BJ, Verbakel WF. Deep Learning-Based Delineation of Head and Neck Organs at Risk: Geometric and Dosimetric Evaluation. *Int J Radiat Oncol Biol Phys* 2019; **104**: 677-684 [PMID: 30836167 DOI: 10.1016/j.ijrobp.2019.02.040]

31 **Loap P**, Tkatchenko N, Kirova Y. Evaluation of a delineation software for cardiac atlas-based autosegmentation: An example of the use of artificial intelligence in modern radiotherapy. *Cancer Radiother* 2020; **24**: 826-833 [PMID: 33144062 DOI: 10.1016/j.canrad.2020.04.012]

32 **Feng X**, Qing K, Tustison NJ, Meyer CH, Chen Q. Deep convolutional neural network for segmentation of thoracic organs-at-risk using cropped 3D images. *Med Phys* 2019; **46**: 2169-2180 [PMID: 30830685 DOI: 10.1002/mp.13466]

33 **Zhang T**, Yang Y, Wang J, Men K, Wang X, Deng L, Bi N. Comparison between atlas and convolutional neural network based automatic segmentation of multiple organs at risk in non-small cell lung cancer. *Medicine (Baltimore)* 2020; **99**: e21800 [PMID: 32846816 DOI: 10.1097/MD.0000000000021800]

34 **Vu CC**, Siddiqui ZA, Zamdborg L, Thompson AB, Quinn TJ, Castillo E, Guerrero TM. Deep convolutional neural networks for automatic segmentation of thoracic organs-at-risk in radiation oncology - use of non-domain transfer learning. *J Appl Clin Med Phys* 2020; **21**: 108-113 [PMID: 32602187 DOI: 10.1002/acm2.12871]

35 **Liu Z**, Liu X, Xiao B, Wang S, Miao Z, Sun Y, Zhang F. Segmentation of organs-at-risk in cervical cancer CT images with a convolutional neural network. *Phys Med* 2020; **69**: 184-191 [PMID: 31918371 DOI: 10.1016/j.ejmp.2019.12.008]

36 **Ahn SH**, Yeo AU, Kim KH, Kim C, Goh Y, Cho S, Lee SB, Lim YK, Kim H, Shin D, Kim T, Kim TH, Youn SH, Oh ES, Jeong JH. Comparative clinical evaluation of atlas and deep-learning-based auto-segmentation of organ structures in liver cancer. *Radiat Oncol* 2019; **14**: 213 [PMID: 31775825 DOI: 10.1186/s13014-019-1392-z]

37 **La Macchia M**, Fellin F, Amichetti M, Cianchetti M, Gianolini S, Paola V, Lomax AJ, Widesott L. Systematic evaluation of three different commercial software solutions for automatic segmentation for adaptive therapy in head-and-neck, prostate and pleural cancer. *Radiat Oncol* 2012; **7**: 160 [PMID: 22989046 DOI: 10.1186/1748-717X-7-160]

38 **Chao KS**, Bhide S, Chen H, Asper J, Bush S, Franklin G, Kavadi V, Liengswangwong V, Gordon W, Raben A, Strasser J, Koprowski C, Frank S, Chronowski G, Ahamad A, Malyapa R, Zhang L, Dong L. Reduce in variation and improve efficiency of target volume delineation by a computer-assisted system using a deformable image registration approach. *Int J Radiat Oncol Biol Phys* 2007; **68**: 1512-1521 [PMID: 17674982 DOI: 10.1016/j.ijrobp.2007.04.037]

39 **Ikushima K**, Arimura H, Jin Z, Yabu-Uchi H, Kuwazuru J, Shioyama Y, Sasaki T, Honda H, Sasaki M. Computer-assisted framework for machine-learning-based delineation of GTV regions on datasets of planning CT and PET/CT images. *J Radiat Res* 2017; **58**: 123-134 [PMID: 27609193 DOI: 10.1093/jrr/rrw082]

40 **Cui Y**, Arimura H, Nakano R, Yoshitake T, Shioyama Y, Yabuuchi H. Automated approach for segmenting gross tumor volumes for lung cancer stereotactic body radiation therapy using CT-based dense V-networks. *J Radiat Res* 2021; **62**: 346-355 [PMID: 33480438 DOI: 10.1093/jrr/rraa132]

41 **Zhong Z**, Kim Y, Plichta K, Allen BG, Zhou L, Buatti J, Wu X. Simultaneous cosegmentation of tumors in PET-CT images using deep fully convolutional networks. *Med Phys* 2019; **46**: 619-633 [PMID: 30537103 DOI: 10.1002/mp.13331]

42 **Kawata Y**, Arimura H, Ikushima K, Jin Z, Morita K, Tokunaga C, Yabu-Uchi H, Shioyama Y, Sasaki T, Honda H, Sasaki M. Impact of pixel-based machine-learning techniques on automated frameworks for delineation of gross tumor volume regions for stereotactic body radiation therapy. *Phys Med* 2017; **42**: 141-149 [PMID: 29173908 DOI: 10.1016/j.ejmp.2017.08.012]

43 **Li S**, Xiao J, He L, Peng X, Yuan X. The Tumor Target Segmentation of Nasopharyngeal Cancer in CT Images Based on Deep Learning Methods. *Technol Cancer Res Treat* 2019; **18**: 1533033819884561 [PMID: 31736433 DOI: 10.1177/1533033819884561]

44 **Ma Z**, Zhou S, Wu X, Zhang H, Yan W, Sun S, Zhou J. Nasopharyngeal carcinoma segmentation based on enhanced convolutional neural networks using multi-modal metric learning. *Phys Med Biol* 2019; **64**: 025005 [PMID: 30524024 DOI: 10.1088/1361-6560/aaf5da]

45 **Zhao L**, Lu Z, Jiang J, Zhou Y, Wu Y, Feng Q. Automatic Nasopharyngeal Carcinoma Segmentation Using Fully Convolutional Networks with Auxiliary Paths on Dual-Modality PET-CT Images. *J Digit Imaging* 2019; **32**: 462-470 [PMID: 30719587 DOI: 10.1007/s10278-018-00173-0]

46 **Guo Z**, Guo N, Gong K, Zhong S, Li Q. Gross tumor volume segmentation for head and neck cancer radiotherapy using deep dense multi-modality network. *Phys Med Biol* 2019; **64**: 205015 [PMID: 31514173 DOI: 10.1088/1361-6560/ab440d]

47 **Men K**, Chen X, Zhang Y, Zhang T, Dai J, Yi J, Li Y. Deep Deconvolutional Neural Network for Target Segmentation of Nasopharyngeal Cancer in Planning Computed Tomography Images. *Front Oncol* 2017; **7**: 315 [PMID: 29376025 DOI: 10.3389/fonc.2017.00315]

48 **Agn M**, Munck Af Rosenschöld P, Puonti O, Lundemann MJ, Mancini L, Papadaki A, Thust S, Ashburner J, Law I, Van Leemput K. A modality-adaptive method for segmenting brain tumors and organs-at-risk in radiation therapy planning. *Med Image Anal* 2019; **54**: 220-237 [PMID: 30952038 DOI: 10.1016/j.media.2019.03.005]

49 **Estienne T**, Lerousseau M, Vakalopoulou M, Alvarez Andres E, Battistella E, Carré A, Chandra S, Christodoulidis S, Sahasrabudhe M, Sun R, Robert C, Talbot H, Paragios N, Deutsch E. Deep Learning-Based Concurrent Brain Registration and Tumor Segmentation. *Front Comput Neurosci* 2020; **14**: 17 [PMID: 32265680 DOI: 10.3389/fncom.2020.00017]

50 **Liu Y**, Stojadinovic S, Hrycushko B, Wardak Z, Lau S, Lu W, Yan Y, Jiang SB, Zhen X, Timmerman R, Nedzi L, Gu X. A deep convolutional neural network-based automatic delineation strategy for

multiple brain metastases stereotactic radiosurgery. *PLoS One* 2017; **12**: e0185844 [PMID: 28985229 DOI: 10.1371/journal.pone.0185844]

51 **Jeong J**, Lei Y, Kahn S, Liu T, Curran WJ, Shu HK, Mao H, Yang X. Brain tumor segmentation using 3D Mask R-CNN for dynamic susceptibility contrast enhanced perfusion imaging. *Phys Med Biol* 2020; **65**: 185009 [PMID: 32674075 DOI: 10.1088/1361-6560/aba6d4]

52 **Charron O**, Lallement A, Jarnet D, Noblet V, Clavier JB, Meyer P. Automatic detection and segmentation of brain metastases on multimodal MR images with a deep convolutional neural network. *Comput Biol Med* 2018; **95**: 43-54 [PMID: 29455079 DOI: 10.1016/j.compbiomed.2018.02.004]

53 **Tang F**, Liang S, Zhong T, Huang X, Deng X, Zhang Y, Zhou L. Postoperative glioma segmentation in CT image using deep feature fusion model guided by multi-sequence MRIs. *Eur Radiol* 2020; **30**: 823-832 [PMID: 31650265 DOI: 10.1007/s00330-019-06441-z]

54 **Meng L**, Tian Y, Bu S. Liver tumor segmentation based on 3D convolutional neural network with dual scale. *J Appl Clin Med Phys* 2020; **21**: 144-157 [PMID: 31793212 DOI: 10.1002/acm2.12784]

55 **Eppenhof KAJ**, Maspero M, Savenije MHF, de Boer JCJ, van der Voort van Zyp JRN, Raaymakers BW, Raaijmakers AJE, Veta M, van den Berg CAT, Pluim JPW. Fast contour propagation for MR-guided prostate radiotherapy using convolutional neural networks. *Med Phys* 2020; **47**: 1238-1248 [PMID: 31876300 DOI: 10.1002/mp.13994]

56 **Elguindi S**, Zelefsky MJ, Jiang J, Veeraraghavan H, Deasy JO, Hunt MA, Tyagi N. Deep learning-based auto-segmentation of targets and organs-at-risk for magnetic resonance imaging only planning of prostate radiotherapy. *Phys Imaging Radiat Oncol* 2019; **12**: 80-86 [PMID: 32355894 DOI: 10.1016/j.phro.2019.11.006]

57 **Torheim T**, Malinen E, Hole KH, Lund KV, Indahl UG, Lyng H, Kvaal K, Futsaether CM. Autodelineation of cervical cancers using multiparametric magnetic resonance imaging and machine learning. *Acta Oncol* 2017; **56**: 806-812 [PMID: 28464746 DOI: 10.1080/0284186X.2017.1285499]

58 **Karimi D**, Zeng Q, Mathur P, Avinash A, Mahdavi S, Spadinger I, Abolmaesumi P, Salcudean SE. Accurate and robust deep learning-based segmentation of the prostate clinical target volume in ultrasound images. *Med Image Anal* 2019; **57**: 186-196 [PMID: 31325722 DOI: 10.1016/j.media.2019.07.005]

59 **Men K**, Dai J, Li Y. Automatic segmentation of the clinical target volume and organs at risk in the planning CT for rectal cancer using deep dilated convolutional neural networks. *Med Phys* 2017; **44**: 6377-6389 [PMID: 28963779 DOI: 10.1002/mp.12602]

60 **Men K**, Zhang T, Chen X, Chen B, Tang Y, Wang S, Li Y, Dai J. Fully automatic and robust segmentation of the clinical target volume for radiotherapy of breast cancer using big data and deep learning. *Phys Med* 2018; **50**: 13-19 [PMID: 29891089 DOI: 10.1016/j.ejmp.2018.05.006]

61 **Zhu J**, Liu X, Chen L. A preliminary study of a photon dose calculation algorithm using a convolutional neural network. *Phys Med Biol* 2020; **65**: 20NT02 [PMID: 33063695 DOI: 10.1088/1361-6560/abb1d7]

62 **Zhang J**, Liu S, Yan H, Li T, Mao R, Liu J. Predicting voxel-level dose distributions for esophageal radiotherapy using densely connected network with dilated convolutions. *Phys Med Biol* 2020; **65**: 205013 [PMID: 32698170 DOI: 1088/1361-6560/aba87b]

63 **Liu Z**, Fan J, Li M, Yan H, Hu Z, Huang P, Tian Y, Miao J, Dai J. A deep learning method for prediction of three-dimensional dose distribution of helical tomotherapy. *Med Phys* 2019; **46**: 1972-1983 [PMID: 30870586 DOI: 10.1002/mp.13490]

64 **Fan J**, Wang J, Chen Z, Hu C, Zhang Z, Hu W. Automatic treatment planning based on three-dimensional dose distribution predicted from deep learning technique. *Med Phys* 2019; **46**: 370-381 [PMID: 30383300 DOI: 10.1002/mp.13271]

65 **Ma M**, Kovalchuk N, Buyyounouski MK, Xing L, Yang Y. Dosimetric features-driven machine learning model for DVH prediction in VMAT treatment planning. *Med Phys* 2019; **46**: 857-867 [PMID: 30536442 DOI: 10.1002/mp.13334]

66 **Valdes G**, Simone CB 2nd, Chen J, Lin A, Yom SS, Pattison AJ, Carpenter CM, Solberg TD. Clinical decision support of radiotherapy treatment planning: A data-driven machine learning strategy for patient-specific dosimetric decision making. *Radiother Oncol* 2017; **125**: 392-397 [PMID: 29162279 DOI: 10.1016/j.radonc.2017.10.014]

67 **Mahdavi SR**, Tavakol A, Sanei M, Molana SH, Arbabi F, Rostami A, Barimani S. Use of artificial neural network for pretreatment verification of intensity modulation radiation therapy fields. *Br J Radiol* 2019; **92**: 20190355 [PMID: 31317765 DOI: 10.1259/bjr.20190355]

68 **Yan H**, Dai JR. Intelligence-guided beam angle optimization in treatment planning of intensity-modulated radiation therapy. *Phys Med* 2016; **32**: 1292-1301 [PMID: 27344457 DOI: 10.1016/j.ejmp.2016.06.005]

69 **Amit G**, Purdie TG, Levinshtein A, Hope AJ, Lindsay P, Marshall A, Jaffray DA, Pekar V. Automatic learning-based beam angle selection for thoracic IMRT. *Med Phys* 2015; **42**: 1992-2005 [PMID: 25832090 DOI: 10.1118/1.4908000]

70 **Sakata Y**, Hirai R, Kobuna K, Tanizawa A, Mori S. A machine learning-based real-time tumor tracking system for fluoroscopic gating of lung radiotherapy. *Phys Med Biol* 2020; **65**: 085014 [PMID: 32097899 DOI: 10.1088/1361-6560/ab79c5]

71 **Guidi G**, Maffei N, Meduri B, D'Angelo E, Mistretta GM, Ceroni P, Ciarmatori A, Bernabei A, Maggi S, Cardinali M, Morabito VE, Rosica F, Malara S, Savini A, Orlandi G, D'Ugo C, Bunkheila F, Bono M, Lappi S, Blasi C, Lohr F, Costi T. A machine learning tool for re-planning and adaptive RT:

A multicenter cohort investigation. *Phys Med* 2016; **32**: 1659-1666 [PMID: 27765457 DOI: 10.1016/j.ejmp.2016.10.005]

72 **Valdes G**, Morin O, Valenciaga Y, Kirby N, Pouliot J, Chuang C. Use of TrueBeam developer mode for imaging QA. *J Appl Clin Med Phys* 2015; **16**: 322-333 [PMID: 26219002 DOI: 10.1120/jacmp.v16i4.5363]

73 **Li Q**, Chan MF. Predictive time-series modeling using artificial neural networks for Linac beam symmetry: an empirical study. *Ann N Y Acad Sci* 2017; **1387**: 84-94 [PMID: 27627049 DOI: 10.1111/nyas.13215]

74 **Valdes G**, Scheuermann R, Hung CY, Olszanski A, Bellerive M, Solberg TD. A mathematical framework for virtual IMRT QA using machine learning. *Med Phys* 2016; **43**: 4323 [PMID: 27370147 DOI: 10.1118/1.4953835]

75 **Valdes G**, Chan MF, Lim SB, Scheuermann R, Deasy JO, Solberg TD. IMRT QA using machine learning: A multi-institutional validation. *J Appl Clin Med Phys* 2017; **18**: 279-284 [PMID: 28815994 DOI: 10.1002/acm2.12161]

76 **Carlson JN**, Park JM, Park SY, Park JI, Choi Y, Ye SJ. A machine learning approach to the accurate prediction of multi-leaf collimator positional errors. *Phys Med Biol* 2016; **61**: 2514-2531 [PMID: 26948678 DOI: 10.1088/0031-9155/61/6/2514]

77 **Granville DA**, Sutherland JG, Belec JG, La Russa DJ. Predicting VMAT patient-specific QA results using a support vector classifier trained on treatment plan characteristics and linac QC metrics. *Phys Med Biol* 2019; **64**: 095017 [PMID: 30921785 DOI: 10.1088/1361-6560/ab142e]

78 **Boon IS**, Au Yong TPT, Boon CS. Assessing the Role of Artificial Intelligence (AI) in Clinical Oncology: Utility of Machine Learning in Radiotherapy Target Volume Delineation. *Medicines (Basel)* 2018; **5** [PMID: 30544901 DOI: 10.3390/medicines5040131]

79 **Guidi G**, Maffei N, Vecchi C, Gottardi G, Ciarmatori A, Mistretta GM, Mazzeo E, Giacobazzi P, Lohr F, Costi T. Expert system classifier for adaptive radiation therapy in prostate cancer. *Australas Phys Eng Sci Med* 2017; **40**: 337-348 [PMID: 28290067 DOI: 10.1007/s13246-017-0535-5]

80 **Tseng HH**, Luo Y, Cui S, Chien JT, Ten Haken RK, Naqa IE. Deep reinforcement learning for automated radiation adaptation in lung cancer. *Med Phys* 2017; **44**: 6690-6705 [PMID: 29034482 DOI: 10.1002/mp.12625]

81 **Varfalvy N**, Piron O, Cyr MF, Dagnault A, Archambault L. Classification of changes occurring in lung patient during radiotherapy using relative γ analysis and hidden Markov models. *Med Phys* 2017; **44**: 5043-5050 [PMID: 28744863 DOI: 10.1002/mp.12488]

82 **Oakden-Rayner L**, Carneiro G, Bessen T, Nascimento JC, Bradley AP, Palmer LJ. Precision Radiology: Predicting longevity using feature engineering and deep learning methods in a radiomics framework. *Sci Rep* 2017; **7**: 1648 [PMID: 28490744 DOI: 10.1038/s41598-017-01931-w]

83 **Lao J**, Chen Y, Li ZC, Li Q, Zhang J, Liu J, Zhai G. A Deep Learning-Based Radiomics Model for Prediction of Survival in Glioblastoma Multiforme. *Sci Rep* 2017; **7**: 10353 [PMID: 28871110 DOI: 10.1038/s41598-017-10649-8]

84 **Li Z**, Wang Y, Yu J, Guo Y, Cao W. Deep Learning based Radiomics (DLR) and its usage in noninvasive IDH1 prediction for low grade glioma. *Sci Rep* 2017; **7**: 5467 [PMID: 28710497 DOI: 10.1038/s41598-017-05848-2]

85 **Cha KH**, Hadjiiski L, Chan HP, Weizer AZ, Alva A, Cohan RH, Caoili EM, Paramagul C, Samala RK. Bladder Cancer Treatment Response Assessment in CT using Radiomics with Deep-Learning. *Sci Rep* 2017; **7**: 8738 [PMID: 28821822 DOI: 10.1038/s41598-017-09315-w]

86 **Siegel RL**, Miller KD, Jemal A. Cancer statistics, 2019. *CA Cancer J Clin* 2019; **69**: 7-34 [PMID: 30620402 DOI: 10.3322/caac.21551]

87 **DeSantis CE**, Miller KD, Dale W, Mohile SG, Cohen HJ, Leach CR, Goding Sauer A, Jemal A, Siegel RL. Cancer statistics for adults aged 85 years and older, 2019. *CA Cancer J Clin* 2019; **69**: 452-467 [PMID: 31390062 DOI: 10.3322/caac.21577]

88 **Akcay M**, Etiz D, Celik O, Ozen A. Evaluation of Prognosis in Nasopharyngeal Cancer Using Machine Learning. *Technol Cancer Res Treat* 2020; **19**: 1533033820909829 [PMID: 32138606 DOI: 10.1177/1533033820909829]

89 **Sepheri S**, Upadhaya T, Desseroit MC, Visvikis D, Le Rest CC, Hatt M. Comparison of machine learning algorithms for building prognostic models in non-small cell lung cancer using clinical and radiomics features from 18F-FDG PET/CT images. *J Nucl Med* 2018; **59**: 328

90 **Zhang S**, Xu Y, Hui X, Yang F, Hu Y, Shao J, Liang H, Wang Y. Improvement in prediction of prostate cancer prognosis with somatic mutational signatures. *J Cancer* 2017; **8**: 3261-3267 [PMID: 29158798 DOI: 10.7150/jca.21261]

91 **Hasnain Z**, Mason J, Gill K, Miranda G, Gill IS, Kuhn P, Newton PK. Machine learning models for predicting post-cystectomy recurrence and survival in bladder cancer patients. *PLoS One* 2019; **14**: e0210976 [PMID: 30785915 DOI: 10.1371/journal.pone.0210976]

92 **Akcay M**, Etiz D, Celik O. Prediction of Survival and Recurrence Patterns by Machine Learning in Gastric Cancer Cases Undergoing Radiation Therapy and Chemotherapy. *Adv Radiat Oncol* 2020; **5**: 1179-1187 [PMID: 33305079 DOI: 10.1016/j.adro.2020.07.007]

93 **Pham TD**, Fan C, Zhang H, Sun XF. Artificial intelligence-based 5-year survival prediction and prognosis of DNp73 expression in rectal cancer patients. *Clin Transl Med* 2020; **10**: e159 [PMID: 32898334 DOI: 10.1002/ctm2.159]

Artificial Intelligence in Medical Imaging

Submit a Manuscript: https://www.f6publishing.com

Artif Intell Med Imaging 2021 April 28; 2(2): 32-36

DOI: 10.35711/aimi.v2.i2.32

ISSN 2644-3260 (online)

MINIREVIEWS

Intrathyroidal ectopic thymus: Ultrasonographic features and differential diagnosis

Erdal Karavas, Oguzhan Tokur, Sonay Aydın, Dilek Gokharman, Cigdem Uner

ORCID number: Erdal Karavas 0000-0001-6649-3256; Oguzhan Tokur 0000-0003-3319-6663; Sonay Aydın 0000-0002-3812-6333; Dilek Gokharman 0000-0003-1166-0576; Cigdem Uner 0000-0002-4846-7764.

Author contributions: Karavas E, Tokur O, Aydin S, Gokharman D, Uner C contribute to the conceptualization, methodology, supervision, and the manuscript writing, review and editing; Karavas E, Tokur O, Aydin S contribute to the data curation, software; Karavas E, Tokur O, Gokharman D, Uner C contribute to the validation; Karavas E, Tokur O, Uner C contribute to the visualization; Karavas E, Tokur O, Aydin S, Gokharman D contribute to the writing, original draft of the manuscript.

Conflict-of-interest statement: The authors declare no conflict of interest.

Open-Access: This article is an open-access article that was selected by an in-house editor and fully peer-reviewed by external reviewers. It is distributed in accordance with the Creative Commons Attribution NonCommercial (CC BY-NC 4.0) license, which permits others to distribute, remix, adapt, build upon this work non-commercially, and license their derivative works

Erdal Karavas, Sonay Aydın, Department of Radiology, Erzincan Binali Yildirim University, Erzincan 24100, Turkey

Oguzhan Tokur, Dilek Gokharman, Department of Radiology, Ankara Training and Research Hospital, Ankara 06230, Turkey

Cigdem Uner, Department of Child Radiology, Ankara Sami Ulus Training and Research Hospital, Ankara 06560, Turkey

Corresponding author: Erdal Karavas, MD, MSc, Associate Professor, Department of Radiology, Erzincan Binali Yildirim University, Yalnızbağ Yerleşkesi, Erzincan 24100, Turkey. erdalkaravas@hotmail.com

Abstract

Intrathyroidal ectopic thymus (IET) is defined as an ectopic thymus tissue that is generally found incidentally and rarely in the thyroid gland in the pediatric group. It occurs as a result of disruption of the embryological migration path and the settling of the thymus tissue into the thyroid gland. In the differential diagnosis, it is mostly confused with thyroid nodules. Although thyroid nodules are less common in children than adults, the rate of malignancy is much higher. Therefore, knowing the general ultrasound findings of IET better may prevent unnecessary invasive attempts and surgical procedures. In this article, we tried to compile the key imaging findings of IET.

Key Words: Thymus; Intrathyroidal thymus; Ultrasonography; Diagnosis

©The Author(s) 2021. Published by Baishideng Publishing Group Inc. All rights reserved.

Core Tip: The unique ultrasonographic features of intrathyroidal ectopic thymus (IET) can be remembered as; well-circumscribed, hypoechoic eco pattern with linear or punctate echogenic foci resembling thymus, fusiform or oval shape, diameters smaller than 1 cm, location of middle and/or lower 1/3 part of thyroid gland, hypovascularity or avascularity and the same strain ratio values with the surrounding thyroid gland on elastography. Although some studies suggested cytopathological examination for the accurate diagnosis of a suspected IET case, majority of the previous studies stated that IET can be followed without the presence of any atypical findings. So that,

on different terms, provided the original work is properly cited and the use is non-commercial. See: http://creativecommons.org/Licenses/by-nc/4.0/

Manuscript source: Invited manuscript

Specialty type: Radiology, nuclear medicine and medical imaging

Country/Territory of origin: Turkey

Peer-review report's scientific quality classification

Grade A (Excellent): 0
Grade B (Very good): B, B, B
Grade C (Good): C
Grade D (Fair): D
Grade E (Poor): 0

Received: March 17, 2021
Peer-review started: March 17, 2021
First decision: March 26, 2021
Revised: March 29, 2021
Accepted: April 20, 2021
Article in press: April 20, 2021
Published online: April 28, 2021

P-Reviewer: Jesus-Silva SG, Madian A, Pekiner FN, Stan F
S-Editor: Wang JL
L-Editor: A
P-Editor: Xing YX

unnecessary surgical or interventional procedures can be avoided.

Citation: Karavas E, Tokur O, Aydın S, Gokharman D, Uner C. Intrathyroidal ectopic thymus: Ultrasonographic features and differential diagnosis. *Artif Intell Med Imaging* 2021; 2(2): 32-36
URL: https://www.wjgnet.com/2644-3260/full/v2/i2/32.htm
DOI: https://dx.doi.org/10.35711/aimi.v2.i2.32

INTRODUCTION

Thyroid lesions in children are mostly in the benign category, but malignant lesions can also be encountered, even rarely. Intrathyroidal ectopic thymus (IET) is a benign lesion that can be encountered in children and does not require treatment. Although it has typical sonographic aspects, it may be misdiagnosed as a thyroid nodule by radiologists who do not have sufficient experience. As a result, a process leading to interventional procedures or even surgery may occur. However, some of its features conflict with thyroid nodules. In these cases, a cytopathological evaluation must be made for the distinction. If IET common ultrasound (US) features are familiarized it can be distinguished from malignant pathologies of the thyroid.

DEVELOPMENT

Thymus tissue develops in the intrauterine 6th week from the 3rd and 4th branchial saccule. Bilaterally developing primordial thymus tissues descend to the anterior mediastinum in the 8th week and combine to form the bilobuled thymus tissue at the 9th week. This descent is from the mandibular angle level to the anterior mediastinum caudally and medially. During migration, the thymic remnant can replace ectopically anywhere along the descent line in the cervical region. Although some articles report that the most ectopic cervical location is intrathyroidal[1], some articles also report it is less common than other ectopic locations in the cervical region[2]. The reason for intrathyroidal localization is thought to be due to the thyroid diverticulum being close to the 3rd branchial sac, although the thyroid tissue basically develops from the 1st and 2nd branchial sac[3].

IET was first described as pathologically by Gilmour in 1937[4]. It does not present with any clinical or physical examination findings in children and is often detected incidentally. Although it is a benign condition, cases showing malignant transformation have been reported in the literature[5]. Its prevalence has been reported between 0.99% and 5.9% in studies[1,4-6]. The mean age of onset varies between 1-10 years in studies[3,5,7,8]. Although not statistically significant, it has been reported slightly more frequently in men[1,3,8].

IET consists of 2 types as abutting and enclosed types, and abutting type is more common than the other. When abutting type is seen, it should be taken into consideration that ectopic thymus tissue may be extending from the anterior mediastinum to the thyroid gland and should be examined carefully[9].

The first diagnostic modality should be US to evaluate the IET and other thyroid lesions[5]. In US, it is observed as a well-circumscribed, hypoechoic lesion containing linear or punctate echogenic foci resembling thymus[1,3,5,7,8,10]. Its contours may be irregular in some cases[8].

Internal punctate echogenicities indicate the Hassall's Corpuscle and their typical histopathological appearance confirms the diagnosis of thymus tissue[10]. Also, because of the similarity of the echo structure and presence of internal echogenic foci, IET can resemble the thymus tissue in the anterior mediastinum[10,11] (Figure 1). When the shape characteristics are examined, IET mostly presents as fusiform or oval[1,3,5,9]. In studies, its dimensions were found to be smaller than 1 cm[3,8,11]. When the location in the thyroid gland is evaluated, it is mostly observed in the middle and lower 1/3 part and more commonly in the posterior parts[1-3,11]. The reason is thought to be that the thymus develops under the pharyngeal sac, where the thyroid develops during embryological development[1]. Only 2 IETs were observed in the upper pole in the study of Erol *et al*[2].

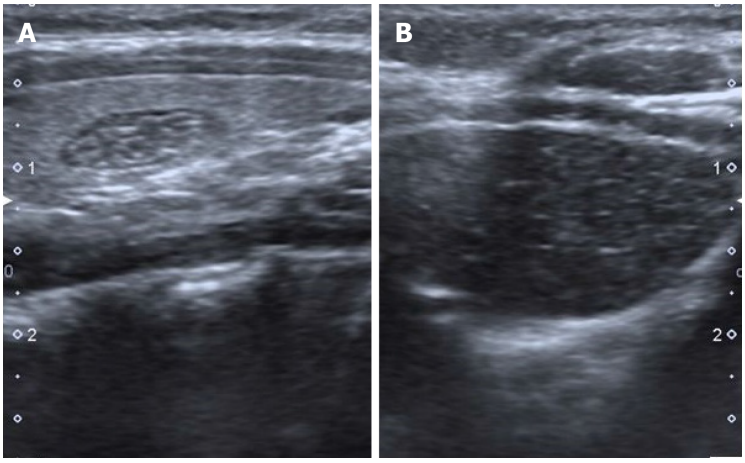

Figure 1 Eight-year-old asymptomatic girl. Longitudinal sonographic images obtained with 7 MHz linear transducer. A: Intrathyroidal ectopic thymus with typical ultrasonographic findings; hypoechoic, fusiform appearance with linear and punctate echogenic focil; B: The resemblance with mediastinal thymic tissue can be seen easily.

In color Doppler examination, IET is hypovascular or avascular compared to surrounding thyroid tissue[1,3,10,11] (Figure 2). Only a few cases have been reported to be isovascular[1,3,11]. Erol *et al*[2] stated that the observation of a vascular structure that passes through the nodule without any compression is a useful hint to differentiate IET and the other nodules.

Elastography was used in two studies, showing that IET had the same stiffness as the surrounding thyroid tissue and the average strain ratio (SR) was defined as 0.99[5,8].

In US follow-up, the dimensions of IET either remain stable or show regression[2,3,12]. Additionally, hormones and enzymes associated with the thyroid gland were also evaluated, and no significant relationship was found with IET[3,5].

In the presence of typical findings of IET described above, absence of palpable thyroid nodule and cervical lymphadenopathy, no prior risk to increased risk of malignancy (radiation exposure to the neck, family history), follow-up will be enough for the management of IET cases[1,2,5,9,10,12]. In the study of Januś *et al*[5], it was underlined that US features of IET can be similar to papillary thyroid cancer (especially diffuse sclerosing variant]. In these cases it can be challenging to differentiate the two entities, and elastography can be helpful[5,8]. Exceptionally, Stasiak *et al*[8] emphasized that cytopathological examination should be performed in cases with suspected IET and the diagnosis could only be reliable in this way[8].

IET is generally confused with thyroid nodules (Figure 3). In pediatric patients, the incidence of thyroid nodules is between 0.2%-1.5%, much less common than adults, but the rate of malignancy is higher[9]. In addition, bilateral lesions in children do not reduce the suspicion of malignancy because thyroid cancer is more common in children when it is multifocal and bilateral[8]. Therefore, further examinations should be made and the distinction between benign and malignant nodules should be revealed. If the ultrasound findings are insufficient for differentiation and the suspicion continues, fine needle aspiration biopsy should be performed first. There are some cases diagnosed by hemi lobectomy in the literature. Although IET is a benign process, it should be known that it may undergo malignant transformation such as thymoma, thymic carcinoma and lymphoblastic lymphoma[5,8]. There are some findings that support the malignant nature of a hypoechoic nodule echo pattern, solid component, ill-defined contour, irregular or round shape, microcalcification, increased vascularity, and pathological lymph node presence[8,9].

Focal thyroiditis is also included in the differential diagnosis. Focal thyroiditis is more hypoechoic and mostly does not contain diffuse echogenic focuses. The contour of focal thyroiditis is ill-defined. Vascularity is also increased (Figure 4)[2].

Intrathyroidal parathyroid gland is similar to IET, but it is differentiated by the absence of echogenic punctate foci. Clinical symptoms and laboratory findings are also useful in differential diagnosis[5].

Intrathyroidal esophageal diverticulum should be considered in differential diagnosis. Its echo pattern is isoechoic or hypoechoic compared to the surrounding thyroid tissue. Internal and peripheral echogenic focuses can be seen. In the differentiation, showing the relationship with the esophagus, changing shape with

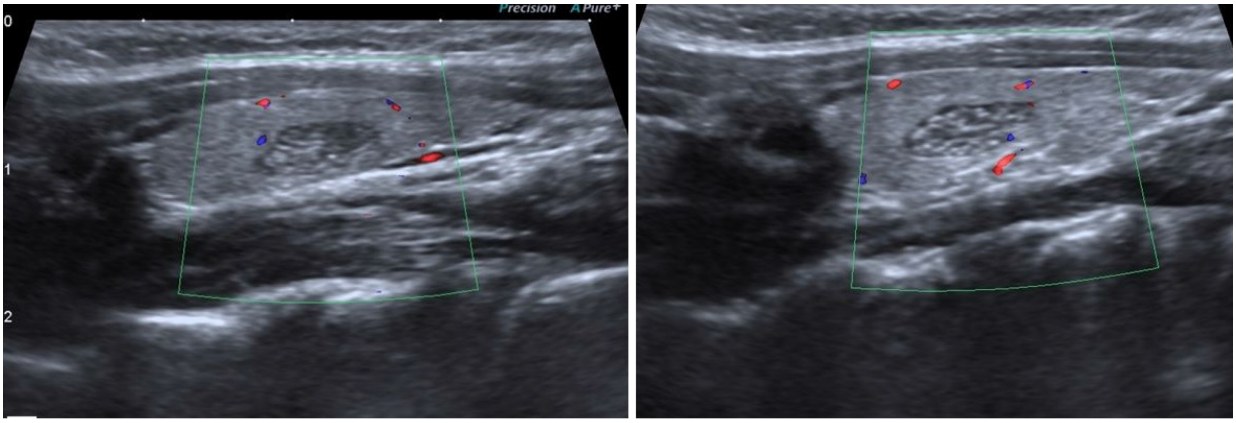

Figure 2 Eight-year-old asymptomatic girl. Longitudinal sonographic images obtained with 7 MHz linear transducer. Both intrathyroidal ectopic thymus cases are hypo vascular in comparison within the surrounding thyroid parenchyma.

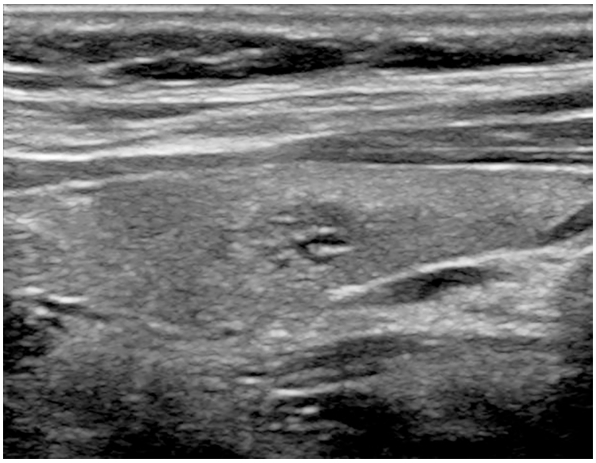

Figure 3 Nine-year-old male with hypothyroidism symptoms. Longitudinal sonographic images obtained with 7 MHz linear transducer. A thyroid nodule presenting with a similar appearance with intrathyroidal ectopic thymus tissue.

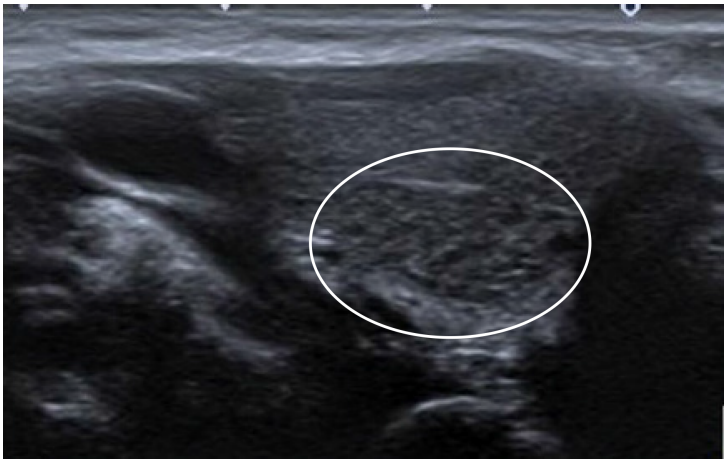

Figure 4 Ten-year-old male with recurrent cough. Longitudinal sonographic images obtained with 7 MHz linear transducer. Abutting type intrathyroidal ectopic thymus. The lesion is located at the lower half of the gland, it has unclear margins. This appearance can be confused with focal thyroiditis.

swallowing and a comet tail artifact due to the inside air can be helpful[1].

Hashimoto thyroiditis nodular form has a solid, hypoechoic echo structure and echogenic punctate focus that can also be observed. It can be well-circumscribed or ill-defined. Laboratory findings may be normal in this type of Hashimoto thyroiditis. Therefore, cytopathological correlation is required[1].

Artificial intelligence (AI) has been playing an increasing role in the diagnosis of thyroidal disease[13], however as far as we know there is not a study concentrating on the use of AI in detecting IET in the English literature.

CONCLUSION

The unique ultrasonographic features of IET can be remembered as well-circumscribed, hypoechoic eco pattern with linear or punctate echogenic foci resembling thymus, fusiform or oval shape, diameters smaller than 1 cm, location of middle and/or lower 1/3 part of thyroid gland, hypovascularity or avascularity and the same SR values with the surrounding thyroid gland on elastography. Although some studies suggested cytopathological examination for the accurate diagnosis of a suspected IET case, most stated that IET can be followed since there is absence of atypical findings. Therefore, unnecessary surgical or interventional procedures can be avoided.

REFERENCES

1 **Yildiz AE**, Elhan AH, Fitoz S. Prevalence and sonographic features of ectopic thyroidal thymus in children: A retrospective analysis. *J Clin Ultrasound* 2018; **46**: 375-379 [PMID: 29575022 DOI: 10.1002/jcu.22590]

2 **Erol OB**, Şahin D, Bayramoğlu Z, Yılmaz R, Akpınar YE, Ünal ÖF, Yekeler E. Ectopic intrathyroidal thymus in children: Prevalence, imaging findings and evolution. *Turk J Pediatr* 2017; **59**: 387-394 [PMID: 29624218 DOI: 10.24953/turkjped.2017.04.004]

3 **Aydin S**, Fatihoglu E, Kacar M. Intrathyroidal ectopic thymus tissue: a diagnostic challenge. *Radiol Med* 2019; **124**: 505-509 [PMID: 30710204 DOI: 10.1007/s11547-019-00987-0]

4 for the Report: "Molecular remission of infant B-ALL after infusion of universal TALEN gene-edited CAR T cells" by W. Qasim, H. Zhan, S. Samarasinghe, S. Adams, P. Amrolia, S. Stafford, K. Butler, C. Rivat, G. Wright, K. Somana, S. Ghorashian, D. Pinner, G. Ahsan, K. Gilmour, G. Lucchini, S. Inglott, W. Mifsud, R. Chiesa, K. S. Peggs, L. Chan, F. Farzeneh, A. J. Thrasher, A. Vora, M. Pule, P. Veys. *Sci Transl Med* 2017; **9** [PMID: 28202780 DOI: 10.1126/scitranslmed.aam9292]

5 **Januś D**, Kalicka-Kasperczyk A, Wójcik M, Drabik G, Starzyk JB. Long-term ultrasound follow-up of intrathyroidal ectopic thymus in children. *J Endocrinol Invest* 2020; **43**: 841-852 [PMID: 31902058 DOI: 10.1007/s40618-019-01172-w]

6 **Fukushima T**, Suzuki S, Ohira T, Shimura H, Midorikawa S, Ohtsuru A, Sakai A, Abe M, Yamashita S, Suzuki S; Thyroid Examination Unit of the Radiation Medical Center for the Fukushima Health Management Survey. Prevalence of ectopic intrathyroidal thymus in Japan: the Fukushima health management survey. *Thyroid* 2015; **25**: 534-537 [PMID: 25778711 DOI: 10.1089/thy.2014.0367]

7 **Bang MH**, Shin J, Lee KS, Kang MJ. Intrathyroidal ectopic thymus in children: A benign lesion. *Medicine (Baltimore)* 2018; **97**: e0282 [PMID: 29620644 DOI: 10.1097/MD.0000000000010282]

8 **Stasiak M**, Adamczewski Z, Stawerska R, Krawczyk T, Tomaszewska M, Lewiński A. Sonographic and Elastographic Features of Extra- and Intrathyroidal Ectopic Thymus Mimicking Malignancy: Differential Diagnosis in Children. *Front Endocrinol (Lausanne)* 2019; **10**: 223 [PMID: 31110490 DOI: 10.3389/fendo.2019.00223]

9 **Yildiz AE**, Ceyhan K, Sıklar Z, Bilir P, Yağmurlu EA, Berberoğlu M, Fitoz S. Intrathyroidal Ectopic Thymus in Children: Retrospective Analysis of Grayscale and Doppler Sonographic Features. *J Ultrasound Med* 2015; **34**: 1651-1656 [PMID: 26269296 DOI: 10.7863/ultra.15.14.10041]

10 **Vlachopapadopoulou EA**, Vakaki M, Karachaliou FE, Kaloumenou I, Kalogerakou K, Gali C, Michalacos S. Ectopic Intrathyroidal Thymus in Childhood: A Sonographic Finding Leading to Misdiagnosis. *Horm Res Paediatr* 2016; **86**: 325-329 [PMID: 27756075 DOI: 10.1159/000450724]

11 **Tritou I**, Raissaki M. Intrathyroidal ectopic thymus tissue: emphasis on details. *Radiol Med* 2019; **124**: 1064-1065 [PMID: 31286340 DOI: 10.1007/s11547-019-01061-5]

12 **Frates MC**, Benson CB, Dorfman DM, Cibas ES, Huang SA. Ectopic Intrathyroidal Thymic Tissue Mimicking Thyroid Nodules in Children. *J Ultrasound Med* 2018; **37**: 783-791 [PMID: 28850707 DOI: 10.1002/jum.14360]

13 **Thomas J**, Haertling T. AIBx, Artificial Intelligence Model to Risk Stratify Thyroid Nodules. *Thyroid* 2020; **30**: 878-884 [PMID: 32013775 DOI: 10.1089/thy.2019.0752]

Artificial Intelligence in Medical Imaging

Submit a Manuscript: https://www.f6publishing.com

Artif Intell Med Imaging 2021 April 28; 2(2): 37-55

DOI: 10.35711/aimi.v2.i2.37

ISSN 2644-3260 (online)

MINIREVIEWS

Current landscape and potential future applications of artificial intelligence in medical physics and radiotherapy

Wing-Yan Ip, Fu-Ki Yeung, Shang-Peng Felix Yung, Hong-Cheung Jeffrey Yu, Tsz-Him So, Varut Vardhanabhuti

ORCID number: Wing-Yan Ip 0000-0002-9118-580X; Fu-Ki Yeung 0000-0003-2721-2356; Shang-Peng Felix Yung 0000-0001-9653-0820; Hong-Cheung Jeffrey Yu 0000-0002-6084-9239; Tsz-Him So 0000-0002-0838-4892; Varut Vardhanabhuti 0000-0001-6677-3194.

Author contributions: Ip WY, Yeung FK, Yung SPF, Yu HCJ, So TH and Vardhanabhuti V contributed to study design, review of literatures, interpretation of data, drafting and revision of the manuscript.

Conflict-of-interest statement: There is no conflict of interest.

Open-Access: This article is an open-access article that was selected by an in-house editor and fully peer-reviewed by external reviewers. It is distributed in accordance with the Creative Commons Attribution NonCommercial (CC BY-NC 4.0) license, which permits others to distribute, remix, adapt, build upon this work non-commercially, and license their derivative works on different terms, provided the original work is properly cited and the use is non-commercial. See: http://creativecommons.org/Licenses/by-nc/4.0/

Manuscript source: Invited

Wing-Yan Ip, Shang-Peng Felix Yung, Varut Vardhanabhuti, Department of Diagnostic Radiology, Li Ka Shing Faculty of Medicine, The University of Hong Kong, Hong Kong SAR, China

Fu-Ki Yeung, Medical Physics and Research Department, The Hong Kong Sanitorium & Hospital, Hong Kong SAR, China and Department of Diagnostic Radiology, Li Ka Shing Faculty of Medicine, The University of Hong Kong, Hong Kong SAR, China

Hong-Cheung Jeffrey Yu, Li Ka Shing Faculty of Medicine, The University of Hong Kong, Hong Kong SAR, China

Tsz-Him So, Department of Clinical Oncology, Li Ka Shing Faculty of Medicine, The University of Hong Kong, Hong Kong SAR, China

Corresponding author: Varut Vardhanabhuti, BSc, MBBS, PhD, Assistant Professor, Department of Diagnostic Radiology, Li Ka Shing Faculty of Medicine, The University of Hong Kong, Room 406, Block K, Pok Fu Lam Road, Hong Kong SAR, China. varv@hku.hk

Abstract

Artificial intelligence (AI) has seen tremendous growth over the past decade and stands to disrupts the medical industry. In medicine, this has been applied in medical imaging and other digitised medical disciplines, but in more traditional fields like medical physics, the adoption of AI is still at an early stage. Though AI is anticipated to be better than human in certain tasks, with the rapid growth of AI, there is increasing concerns for its usage. The focus of this paper is on the current landscape and potential future applications of artificial intelligence in medical physics and radiotherapy. Topics on AI for image acquisition, image segmentation, treatment delivery, quality assurance and outcome prediction will be explored as well as the interaction between human and AI. This will give insights into how we should approach and use the technology for enhancing the quality of clinical practice.

Key Words: Artificial intelligence; Medical physics; Radiotherapy; Image acquisition; Image segmentation; Treatment planning; Treatment delivery; Quality assurance

©The Author(s) 2021. Published by Baishideng Publishing Group Inc. All rights reserved.

manuscript

Specialty type: Oncology

Country/Territory of origin: China

Peer-review report's scientific quality classification
Grade A (Excellent): 0
Grade B (Very good): 0
Grade C (Good): C, C
Grade D (Fair): 0
Grade E (Poor): 0

Received: March 22, 2021
Peer-review started: March 22, 2021
First decision: March 26, 2021
Revised: April 1, 2021
Accepted: April 20, 2021
Article in press: April 20, 2021
Published online: April 28, 2021

P-Reviewer: Jiang Y
S-Editor: Wang JL
L-Editor: A
P-Editor: Xing YX

Core Tip: Artificial intelligence (AI) applications in medical physics and radiotherapy represent an important emerging area in AI applications in medicine. The most notable improvements for the many aspects of radiotherapy are the ability to provide an accurate result with consistency and eliminate inter-and intra-observer variations. Perspectives from physicians and medical physicists about the use of AI are presented, and suggestions of how human can co-exist with AI are made to better equip us for the future.

Citation: Ip WY, Yeung FK, Yung SPF, Yu HCJ, So TH, Vardhanabhuti V. Current landscape and potential future applications of artificial intelligence in medical physics and radiotherapy. *Artif Intell Med Imaging* 2021; 2(2): 37-55
URL: https://www.wjgnet.com/2644-3260/full/v2/i2/37.htm
DOI: https://dx.doi.org/10.35711/aimi.v2.i2.37

INTRODUCTION

Radiotherapy (RT) is an important component of cancer treatment and nearly half of all cancer patients receive RT during their treatment pathways[1]. Increasingly, the use of new technologies such as artificial intelligence (AI) tools plays an important role in RT in various aspects from image acquisition, tumour segmentation, treatment planning, delivery, quality assurance (QA), *etc*. The list will no doubt continue to develop and grow over time as the technology continues to mature. Advancements in computing power and data collection have increased the utilization of AI. The adaptation of a more sophisticated modelling approach has become more widespread creating more accurate predictions. Available datasets from radiation oncology have been generally smaller and more limited than datasets from other medical disciplines such as medical imaging, so the performance of AI is constrained in medical physics disciplines by the available data[2].

According to the data on PubMed search engine performed in Figure 1, which is queried on March 20, 2021, there is a clear increasing trend in AI in the medical literature. Both graphs show an increasing trend but the numbers in medical physics and RT disciplines are several orders of magnitudes lower than in the general medical diagnosis groups. However, the increasing interest in AI applications in medical physics and RT is clear.

In this review article, we will focus on the different aspects of medical physics practice and RT applications and discuss the emerging applications and potentials relating to each area. This is summarised in Figure 2. The structure of this paper is as follows. In section 1, we introduce image synthesis application and benefit in image acquisition. In section 2, we discuss how AI is being used in image segmentation moving from the traditionally manual labour-intensive task to a more automated system. In section 3, we present the function of treatment planning and demonstrate how AI techniques can improve the plan accuracy. In section 4, we describe the benefit in treatment delivery, such as accuracy in position/motion management, organ tracking and dose calculation. In section 5, we explain how AI can be used to improve the performance in the QA process and the advantages of using AI in QA. In section 6, we talk about the prediction of patient outcome and discuss the concerns of patients and clinicians when using AI in the fields that mentioned above. In section 7, we discuss aspects of human-AI interaction. Finally, in section 8, we summarize and evaluate whether AI involved in medical decision making is a benefit or a threat?

IMAGE ACQUISITION

Image synthesis application in RT

RT planning images are used to segment and contour organ at risks (OARs) and target volume (TV), and to plan the treatment. The images require accurate geometric coordinates and excellent image contrast to accurately contour the target in question. A summary, flow chart of image acquisition is shown in Figure 3. The other prerequisites include having a correct electron density of the tissues being imaged to

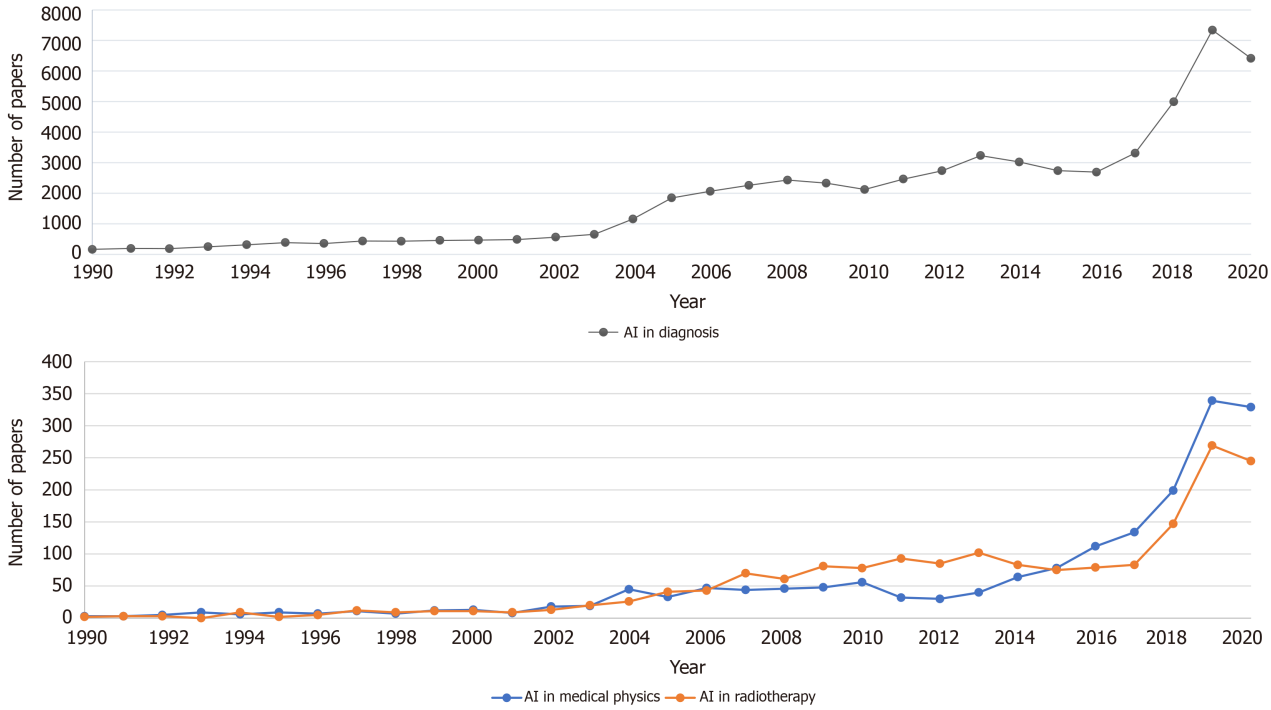

Figure 1 Number of papers in 'Artificial intelligence in diagnosis', 'Artificial intelligence in medical physics', and 'Artificial intelligence in radiotherapy'. AI: Artificial intelligence.

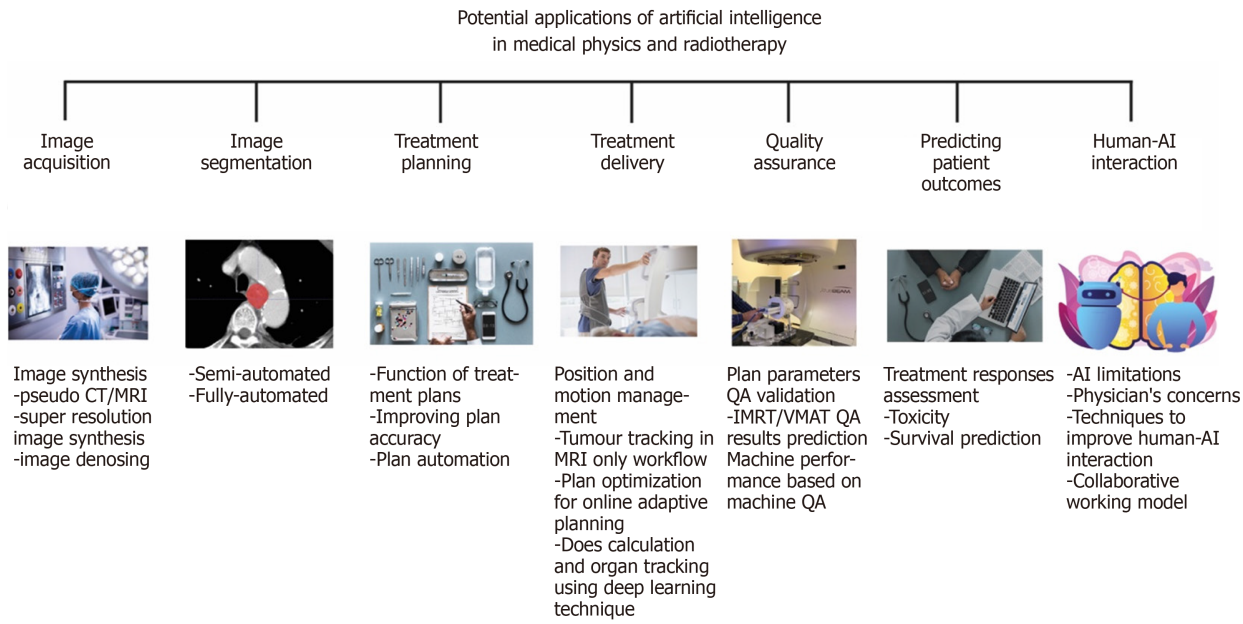

Figure 2 Potential applications of artificial intelligence in medical physics and radiotherapy. AI: Artificial intelligence; QA: Quality assurance; IMRT: Intensity modulated radiotherapy; VMAT: Volumetric-modulated arc therapy; CT: Computed tomography; MRI: Magnetic resonance imaging.

calculate the amount of dose from the treatment beams being attenuated and absorbed by tissues in treatment planning so that an accurate dose can be delivered to the tumour.

Since magnetic resonance imaging (MRI) has advantages in soft tissue contrast for tissues such as brain and prostate (and allows for more accurate lesion localization) but MRI does not have a correlation of electron density in its image. There is a need to fuse the images together with computed tomography (CT) in the current practice. Therefore, when physicians contour on a set of images, the aligned geometric coordinates can ensure a correct contour registration. However, the patient might

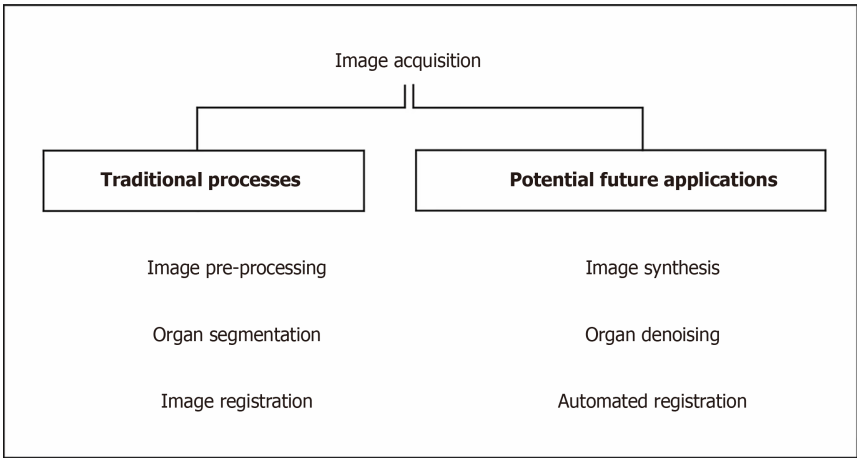

Figure 3 Flow chart of Image processing.

require scanning both MRI and CT image and even the diagnostic PET images beforehand. To reduce the workload or increase the efficiency of those MRI, CT machines, many kinds of image synthesis research have been carrying on based on deep learning technique[3]. The followings are the different applications of image synthesis and advancement using AI as applied to image acquisition. Table 1 summarises the most recent contemporary work.

Pseudo CT/ MRI synthesis

There are several pieces of research on pseudo CT image synthesis from MRI images to help registration of different image modalities or target delineation[4]. Fu *et al*[5] synthesized CT image using cycle consistent generative adversarial network which is an image synthesis network to assist registration of CT-MRI images by directly registering synthetic-CT to original CT images or to have MR-only treatment planning by generating synthetic-CT for treatment planning based on scanned MR image . In addition, Liu *et al*[6,7] researched on generating synthetic-CT from MRI-based treatment planning to derive electron density from routine anatomical MRI so that it can be possible to have MRI-only treatment planning for liver, and prostate cancer.

There is also pseudo MRI synthesis from a CT image for prostate target delineation based on the synthetic MR image from CT image using fully convolution network[8].

Super-resolution image synthesis

To improve the image resolution and quality, Dong *et al*[9] presented a novel super-resolution convolution neural network approach to map between low and high-resolution images in order to synthesize superior-resolution images than other approaches. Bahrami *et al*[10] and Qu *et al*[11] also focus on pseudo synthesis of 7T MRI image from normal 3T MRI using deep learning technique. The high resolution can have a better tissue contrast which can enhance contouring accuracy and on the other hand, will not pose additional dose or scanning time for the patient simulation.

Image denoising

Image denoising is important to improve the signal-to-noise ratio of low-dose CT. Yang *et al*[12] have introduced a CT image denoising method using a generative adversarial network (GAN) with Wasserstein distance and perceptual similarity, so that it can function as conventional CT while keeping a low radiation dose level to the patient. Wang *et al*[13] and Chen *et al*[14] also train the low-dose CT data with a fully convolution neural network with residual blocks and attention gates so to generate a set of data with improved noise, contract-to-noise ratio.

Benefits of using image synthesis technique in RT planning

With the introduction of machine learning and deep learning, various modalities of images can be artificially synthesized for oncologists to take reference, draw different contours on images with superior tissue contrast and fuse together afterwards with the treatment planning software. This can greatly reduce patient scanning time with different modalities. On the other hand, the improvement of images tissue contrast and resolution can help to reduce the margin of the target in order to reduce the

Table 1 Summary of contemporary deep learning methods in image acquisition

Ref.	Architecture	Purpose
Fu *et al*[5], 2020	Cycle consistent generative adversarial network	To enable pseudo CT-aided CT-MRI image registration
Liu *et al*[6], 2019	Cycle generative adversarial network	To derive electron density from routine anatomical MRI for MRI-based SBRT treatment planning
Liu *et al*[7], 2019	3D Cycle-consistent generative adversarial network	To generate pelvic synthetic CT for prostate proton therapy treatment planning
Lei *et al*[8], 2020	Cycle generative adversarial network for synthesis and fully convolution neural network for delineation	To help segment and delineate of prostate target by pseudo MR synthesis from CT
Dong *et al*[9], 2016	Super resolution convolution neural network	To develop novel CNN for high- and low-resolution images mapping
Bahrami *et al*[10], 2016	Convolution neural network	To reconstruct 7T-like super-resolution MRI from 3T MR images
Qu *et al*[11], 2020	Wavelet-based affine transformation layers network	To synthesize superior quality of 7T MRI from its 3T MR images than existing 7T MR images
Yang *et al*[12], 2018	Generative adversarial network with Wasserstein distance and perceptual loss function	To denoise low-dose CT image and improve contrast for lesion detection
Chen *et al*[14], 2017	Deep convolution neural network	To train the mapping between low- and normal-dose images so to efficiently reduce noise in low-dose CT
Wang *et al*[13], 2019	Cycle-consistent adversarial network with residual blocks and attention gates	To improve the contrast-to noise ratio for low-dose CT simulation in brain stereotactic radiosurgery radiation therapy

CNN: Convolutional neural network; CT: Computed tomography; MRI: Magnetic resonance imaging.

uncertainty and improve the dosimetric accuracy of the RT treatment.

IMAGE SEGMENTATION

What is image segmentation?

Image segmentation is an important routine for RT for distinguishing anatomical structures and target[15], as well as comprising sets of pixels[16]. Before the advent of AI, radiation oncologists segment those regions of interest on RT simulation scans (*i.e.*, CT and MRI) manually. They originally used a rigid algorithm and need human interference, professional judgement, and experience. These include thresholding, K-means clustering, histogram-based image segmentation and edge detection[16].

The long duration for manual segmentation is one of the main reasons for the delay in the start of RT treatment, especially in clinics with limited resources. The locoregional control and overall survival rates are lowered because of the inefficiency in the workflow. It also hinders the adaptive RT treatment, because the new images indicating the anatomical changes of the patients have to be segmented for an accurate dose accumulation estimation after each treatment cycle[15].

AI in image segmentation

Accurate segmentation for TV and OARs are necessary for RT plans, but inconsistency such as inter-and intra-observer variability for manual segmentation has been reported. This is because the task is subjective in nature; the decision is made based on an individual's knowledge, judgement and experience. The quantitative and dosimetric analyses are therefore affected, with a varying degree of impact. If an AI tool can be developed with less inherent variability, this would be an invaluable tool for addressing this issue. In order to keep up with modern development, automatic segmentation is needed. It has to overcome image-related problem and provide accurate, efficient and safe RT planning[15].

There are many segmentation types, such as Atlas-based segmentation and Image-based segmentation *etc.* Deep learning in segmentation is a very broad topic, and in broader medical applications, there are several architectures used (Table 1).

The availability of segmented data and computer power were the main reason for manual segmentation in the earlier years. Most segmentation techniques utilised little to no prior knowledge, and these are regarded as low-level segmentation approach.

Examples of these techniques are region growing, heuristic edge detection and intensity thresholding algorithms[15].

Improvement in auto-segmentation

In the past twenty years, a good amount of effort has been poured into the medical imaging field to make use of prior knowledge. Anatomical structures, such as the shape and appearance characteristics are used to compensate for the insufficient soft tissue contrast of CT data, in order to produce an accurate definition of the anatomical boundary[15].

In recent years, deep learning-based software for auto-segmentation has been shown to provide a great leap of improvements over previous approaches. The field of deep learning has become more popular, notably after the seminal paper by Krizhevsky *et al*[17] (2012) which showed a much-improved prediction in image classification and recognition tasks using a deep convolutional neural network (CNN) architecture called AlexNet. More researches followed this approach with the use of a CNN for image segmentation, and the results performed better than prior algorithms, leading to a quick adaptation for deep learning in auto segmentation for medical images[15].

The use of CNNs involves feeding segments of an image as an input, labelling the pixels. The image is scanned by the network, then the network observes the image with a small filter each time until the entire image is mapped[18].

The newest auto-segmentation

Automatic segmentation is usually used in conjunction with manual and semiautomatic segmentation. Manual segmentation requires considerable time and expertise, but often with poor reproducibility. Semiautomatic segmentation relies on human involvement, errors and mistakes can also be expected. Automatic segmentation can provide more accurate results with minimal errors, however, several limitations such as noise existence, partial volume effects, the complexity of three dimensions (3D) spatial multiclass features, spatial and structural variability hinder the effectiveness of automatic segmentation[19].

DeepLab[20], U-Net[21], fully convolutional networks (FCN)[22], dense FCN and residual dense FCN are some of the state-of-the-art neural networks that have been used to tackle this issue. Qayyum *et al*[23] proposed volumetric convolutions for processing 3D input slices as a volume, with no postprocessing steps required. It provided an accurate and robust segmentation that indicated the complete volume of a patient at once.

The test between the proposed model and the current state of the art methods using SegTHOR 2019 dataset was compared. The challenge for this dataset is the position and shape of each organ at each slice has low contrast in CT images as well as the great variation in shape and position. The dataset presented a multiclass problem, and performance metrics are used to evaluate existing deep learning methods and the method proposed by Qayyum *et al*[23] The proposed model provided an improved segmentation performance and produced superior results compared with existing methods.

Limitation in segmentation

The training of deep neural networks (DNNs) for 3D models is challenging, as most deep learning architectures are based on FCN. FCN uses a fixed receptive field and objects with varying size can cause a failure in segmentation. Increasing the field of view and using a sliding window based on complete images can solve the fixed field issue[23].

Several other issues have been reported, such as overfitting, prolonged training time and gradient vanishing. Target organs that do not have a homogeneous appearance and ill-defined borders pose a great challenge to automatic segmentation. In addition, the heterogeneity of appearances even for a single disease entity is a challenge *e.g.*, the appearance of the target could change from patient to patient as well as intra-patient variation between treatment cycles (as if often caused by tumour necrosis). These issues can cause a decrease in performance in 3D deep learning models when handling 3D volumetric datasets. Using an atrous spatial pyramid pooling module with multiscale contextual feature information can assist in handling the issue of changes in sizes, locations and heterogeneous appearances of the target organs and nearby tissues[23].

There is also an issue of paucity of data. A large amount of annotated data is required for training accurate segmentation using deep learning approach.

Increasingly there are several open-source labelled datasets in medical imaging[24-26]. Increasing numbers as well as diversity are needed to increase innovation in this field.

TREATMENT PLANNING

The function of treatment plans

In modern RT, it is crucial to maximize the radiation to the cancer tumour while minimising radiation and potential damage to the surrounding healthy tissues. Intensity modulated RT (IMRT) and volumetric-modulated arc therapy (VMAT) are the two standard treatment techniques for external beam RT treatments that can achieve the tissue-sparing effect while delivering a suitable amount of dose to the planned TV. The treatment plan often involves dose calculations and dose-volume histogram (DVH) which are tools to evaluate the dose to various organs and help the medical staff to determine the quality of the plan. The plans require a lot of time and effort to produce due to the dose constraints and inter-operator variation[27-29].

Methods for improving plan accuracy

Accurate DVH predictions are essential for automated treatment planning, and the predictions keep on improving over the past decade. Concepts such as overlapping volume histogram to describe the geometry of OARs and method for searching similar plans in a clinical database to guide the treatment planning for new patients were proposed. Deep learning methods were used recently to predict the dose distribution in 3D. Because of the nature of DNNs, it relies heavily on the amount and quality of the sample to achieve a high prediction accuracy. The performance could also be affected by parameters such as beam arrangement and voxel spacing in the treatment plan. The robustness of the prediction model can be enhanced with additional pre-processing layers and data augmentation. Through the usage of de-noising auto-encoder for pre-training DNN, more robust feature can be learnt, and less complex neural network can also produce excellent feature fitting capabilities[27].

Benefits provided by automation

Treatment planning is time-consuming, and the method used by each person performing the optimisation can affect the quality of the outcome[30-32]. Automating the treatment planning process can potentially lower the time required for manual labour and reduce the interobserver variations for dose planning. It is generally anticipated that the overall plan quality should improve with the use of AI[32].

The dose objective defined by the dosimetrist determines the dose distribution, usually according to the institution-specific guidelines. However, guidelines cannot provide an optimal dose distribution for specific patients, since the lower achievable dose limit to healthy surrounding tissues for the patient is not known. So, each treatment plan is patient-specific and is produced by trained dosimetrists. Optimisation of the plan is still labour-intensive, it makes it difficult to ensure the clinical treatment plan is properly optimised. All of these concerns lead to the need for automation as a solution to reduce the amount of time spent on the plans and the variations between dosimetrists[32].

The outcome of automated plans

Auto planning software produces comparable or better results for prostate cancer according to Nawa *et al*[28] (2017) and Hazell *et al*[32] (2016). Most OARs receive significant better results with the dose level of the DVHs, and auto planning managed to give clinically acceptable plans for all cases. The results were similar with head and neck cancer treatment. Dosimetrists can potentially have more time to focus on difficult dose planning goals, fine-tuning specific area and spend less time on the mundane tasks of the planning process[32].

TREATMENT DELIVERY

AI in the future will have the ability to accurately identify both normal and TV during treatment and estimates the best modality and beam arrangement from various clinical options. This will lead to an increase in local tumour control and reduces the risk of toxicity to surrounding normal tissue. Integration of clinically relevant data from other

sources in addition will allow AI system to tailor the treatment approach beyond the current state of the art methods. The time burden of human intervention and the time taken for the overall process can be reduced substantially[2].

Position and motion management

Integrated cone-beam CT (CBCT) is commonly used to image the position of the patients. As CBCT has a much lower quality than planning CT images, AI is needed to improve the image quality of CBCT to enable more accurate positioning for treatment[33]. Other imaging techniques such as onboard MRI, ultrasound and infrared surface camera, are used to monitor the motion of the patients as shown in Figure 4. These provide an opportunity for AI to refine and enhance the monitoring during the treatment[34].

The motion of the patient or organ throughout the treatment contributing to inaccuracies in treatment delivery will inevitably increase the radiation dose to surrounding healthy tissues. Motion managements are used for monitoring the extent of the motion from respiration or digestion[35]. There is a potential for the use of AI to predict the diverse variables by creating patient-specific dynamic motion management models[36]. Complex breathing patterns in real-time to accurately track tumour motion are the major task for predictive algorithms[37].

Throughout the treatment, there are changes in the patient's anatomy between the planning appointment and treatment delivery, or even throughout the treatment. Re-planning is necessary when the tumour shrinks or grows, or sometimes with anatomical variations such as the movement of internal organs and gas or liquid filling of the bowels and stomach. Adaptive treatments require a new plan to be created based on up-to-date images of the patient's anatomy. AI tools help predict geometric changes in patient throughout the treatment, thus identify the ideal time point for adaptation[34].

Tumour tracking in MRI only workflow

Apart from conventional cone-beam CT images, AI is involved in the RT treatment for motion tracking using MR images. MRI provides superior soft-tissue contrast compared to conventional CT, and thus target delineation in prostate cancer RT using MRI has become more widespread[38]. However, in RT planning, the combination of MRI and CT image is there is a spatial uncertainty of < 2 mm from the image registration for prostate between MRI and CT[39]. A systematic registration error could lead to an error in treatment, so the dose distribution does not conform to the intended target and results in the tumour control being compromised[40].

As briefly mentioned in section 1, one way to minimize the error is to implement an MRI-only workflow so the plan does not rely on the image from CT scanners. Gold fiducial markers are commonly used in prostate cancer for target positioning, they are detected by using the difference in magnetic susceptibility between the gold markers and the tissue nearby. Multi-echo gradient echo sequence is proposed by Gustafsson *et al*[40] for identifying the fiducial markers. The automatic detection of gold fiducial markers can save time and resources, as well as removing inter-observer differences. From the experiment performed by Gustafsson *et al*[40] and Persson *et al*[41], the true positive detection rates achieved were 97.4% and 99.6% respectively. The results were comparable to manual observer results and they were better than most non deep learning automatic detection methods. A quality control method was also introduced to call upon the attention of the clinical staff when a failure in detection had occurred, which provided a step towards AI automation for MRI-only RT especially for the prostate[40].

Plan optimization for online adaptive planning

Besides monitoring the anatomical changes and motion during treatment, AI is heavily involved in the process of delivery of the treatment beam. VMAT delivery is one of the current standard RT technique. Currently, the treatment plan for VMAT is time-consuming[42]. Machine parameter optimization (MPO) is used to determine the sequence of linac parameters such as multileaf collimators (MLCs) movements, the planning usually involves a manual trial and error approach to determine the best optimizer inputs to obtain an acceptable plan, and execution time for the optimizer is escalated further due to it being run multiple times. There is a need for a fast VMAT MPO algorithm, so while the patient is in the treatment position, the MPO can be executed multiple times for online adaptive planning[43-45].

Reinforcement learning (RL) is a form of machine learning approach, trained to estimate the best sequence of actions to reduce a cost as low as possible in a simulated

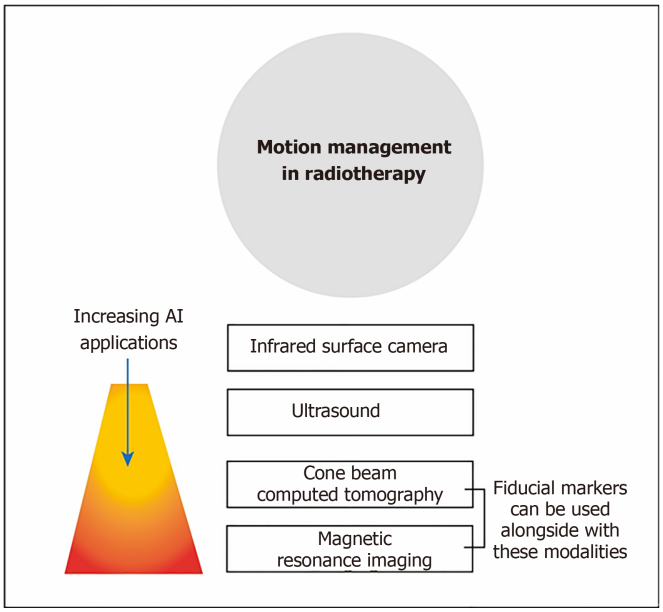

Figure 4 Different strategies used in motion management in radiotherapy. AI: Artificial intelligence.

environment through trial and error. It can be applied to new cases to quickly optimise treatment plans, machine parameters and corresponding dose distributions. The result shows RL VMAT approach produces a rapid and consistent result in both training and test cohort, showing a generalisable machine control policy without notable overfitting in the training cohort despite the small number of patients. The total execution time for plan optimisation was 30 s, with the potential to decrease the time even further because the algorithm can be implemented in parallel across different slices within the plan[45].

Dose calculation and organ tracking using a deep learning technique

Dose calculation of RT treatment using Monte Carlo (MC) simulation is very time consuming[1]. Kernel-based algorithm using DNN proposed by Debus *et al*[46] manages to calculate the peak dose and valley dose in a few minutes with little difference to MC simulation.

Besides the fast calculation speed for dose, kernel-based algorithm is used for identifying the irradiation angle to optimized beam angle for intensity-modulated RT plan. The optimized beam angle spares the organs at risk better in pancreatic and intracranial cancer[47]. It also gives a low-cost computational solution to markerless tracking of tumour motion, such as in kilovoltage fluoroscopy image sequence in image-guided RT (IGRT). The kernel-based algorithm provides a better tracking performance than the conventional template matching method, and it is comparable to the fluoroscopic image sequence[48]. DNN is used to interpret projection X-ray images for markerless prostate localization. The experimental result shows the accuracy is high and can be used for real-time tracking of the prostate and patient positioning[1,49].

QUALITY ASSURANCE

QA is a way to figure out and eliminate errors in radiation planning and delivery but more importantly to ensure consistent quality of the treatment plans. It is an important tool in evaluating the dosimetric and geometric accuracy of the machine and treatment plans. There are a lot of QA researches based on deep learning and machine learning technique[50,51] for improving the accuracy and efficiency of QA procedures. Most adopt a 'human creates while machine verifies' approach. The followings are different sorts of applications of applying AI onto QA in RT. A summary is presented in Table 2.

Plan parameters QA validation

Machine learning can be applied to automated RT plan verification. It aims to verify

Table 2 Summary of contemporary deep learning methods in quality assurance

Ref.	Architecture	Purpose
Chang *et al*[52], 2017	Bayesian network model	To verify and detect external beam radiotherapy physician prescription errors
Kalet *et al*[53], 2015	Bayesian network model	To detect any unusual outliners from treatment plan parameters
Tomori *et al*[54], 2018	Convolutional neural network	To predict gamma evaluation of patient-specific QA in prostate treatment planning
Nyflot *et al*[55], 2019	Convolutional neural network	To detect the presence of introduced RT delivery errors from patient-specific IMRT QA gamma images
Granville *et al*[56], 2019	Support vector classifier	To predict VMAT patient-specific QA results
Li *et al*[57], 2017	ANNs and ARMA time-series prediction modelling	To evaluate the prediction ability of Linac's dosimetry trends from routine machine data for two methods (ANNs and ARMA)

QA: Quality assurance; RT: Radiotherapy; IMRT: Intensity modulated radiotherapy; VMAT: Volumetric-modulated arc therapy; ANNs: Artificial neural networks; ARMA: Autoregressive moving average.

the human-created treatment plan to eliminate any outliners in plan parameters, error-containing contours. Chang *et al*[52] developed a Bayesian network model to detect external beam RT physician order errors ranging from total prescription dose, modality, patient setup options so that these errors can be figured out and rectified as soon as possible without undergoing re-simulation and re-planning. Kalet *et al*[53] further investigated around 5000 prescription treatment plans within 5 years and construct a Bayesian learning model for estimating the probability of different RT parameters from given clinical information. It can act as a database to cross-reference with existing physicians' prescription, for example, to safeguard against human errors, *e.g.*, new doctors. However, such QA checking does not mean to override some exceptional case/physicians' decisions but acts as supporting information as a safety net.

IMRT/VMAT QA results prediction

Patient-specific QA is time-consuming, but this is the most direct and comprehensive way to validate an IMRT or VMAT plan that uses sophisticated MLC patterns. Tomori *et al*[54] made use of a CNN network to predict and estimate the gamma passing rate of these planning plans for prostate cancer based on input training data (volume of planning TV and rectum, monitor unit values of individual field). In the future, patient-specific QA can hopefully be fully automated. Nyflot *et al*[55] also use a CNN with triplet learning to extract the features from IMRT QA gamma comparison results and train the model to distinguish any introduced RT treatment delivery errors like MLC mispositioning error just based on QA gamma results.

Granville *et al*[56] also trained a linear support vector classifier to predict the VMAT QA measurements results based on training measured dose distribution using biplanar diode arrays.

Machine performance prediction based on machine QA

To ensure the accuracy and stability of the treatment machine and plans, sufficient QA tests ought to be performed. Kalet *et al*[50] highlighted that by using machine performance and regular QA measurement logs as input, it can train the model to predict machine performance so as to trigger any preventive maintenance from the service engineers or save time spent to perform additional routine machine QAs.

Li *et al*[57] have used longitudinal daily Linear accelerator (Linac) QA results over 5 years to build and train the model using artificial neural networks or autoregressive moving average time-series prediction modelling techniques so to help understand Linac's behaviour over time and predict the trends in the output[57]. In the future, timely preventive maintenance can be scheduled if necessary after prediction.

The benefit of AI in QA

Chan *et al*[51] highlighted currently many research applications of AI in RT QA focused on predicting the machine performance and patient-specific QA passing rate results. These QA prediction tools based on deep and machine learning can be

incorporated into the treatment planning optimiser so that has a timely prediction of QA gamma rate before finalizing the plan. It minimises time spent on repeating measurement/replanning in case of failing QA tests. By monitoring the machine output performance, it can also help to give feedback to the treatment planning system to improve the accuracy of planning.

PREDICTING PATIENT OUTCOMES

AI also has a role in following outcomes of patients being treated with RT. Many prediction models have been developed, which can be organised by the outcomes predicted as well as the methods used. For RT, the main outcomes that have been investigated are treatment response (*e.g.*, local tumour control and survival) and toxicity. However, the methods used to make these predictions vary widely based on the available data. As studies often acquire these data points retrospectively, the availability of 'ground truth' data may vary according to the clinical setting. To reflect the heterogeneity of data used in some studies, for example, Xu *et al*[58] predicted the chemoRT response of NSCLC patients using 2 datasets. The first set did not have surgery, whereas the second set required surgery and thereby providing data for the pathologic response.

Studies also required data in varying quantity. Various combinations of clinical, imaging, dosimetry, pathological, genomic data have been used to generate the models. Longitudinal data is also important, as shown by Shi *et al*[59] using both a pre-treatment and mid radiation MRI to predict chemoradiation therapy response in rectal cancer . To overcome, difficulties of acquiring large amounts of medical data, techniques such as transfer learning has been used to allow algorithms to train on separate large data sets[60].

The outcome predicted: Treatment response assessment

Tumor control occurs when the appropriate dose is delivered to the tumor, leading to a reduction in the growth of the tumor. It can be assessed grossly by the degree to which the tumor's size changes. Increasingly, changes have been assessed at a more microscopic level based on imaging characteristics (*e.g.*, functional imaging and quantitative analysis such as radiomics). It can also be conceptualized over multiple time points, ranging from the initial treatment response to recurrence, and to the overall survival.

For example, Mizutani *et al*[61] used clinical variables and dosimetry to predict the overall survival of malignant glioma patients after RT using SVM. Oikonomou *et al*[62] analyzed radiomics of PET/CT to predict recurrence and survival after SBRT for lung cancer. Regarding treatment failure, Aneja *et al*[63] used a DNN to predict the local failure over 2 years after SBRT for NSCLC, while Zhou *et al*[64] predicted the distant failure after SBRT for NSCLC using SVM . In shorter time frames, Wang *et al*[65] predicted the anatomic evolution of lung tumors halfway through the 6-wk course of RT using a CNN. Furthermore, Tseng *et al*[66] used RL to allow 'adaptation' of RT to the tumor response. Several studies have also examined treatment response in terms of prediction of pathological response following neoadjuvant chemotherapy using pre-treatment CT scans using radiomics with machine learning classification[67,68].

There are several studies utilising machine learning and AI in the task of prognostication. For example, a multi-centre study using a radiomics approach was utilised in predicting recurrence-free survival in nasopharyngeal carcinoma using MRI data[69]. In this study, an attempt was also made to explain the model using SHAP analysis which could help derive feature importance used in the predictive model.

The outcome predicted: Toxicity

Radiation toxicity is the other outcome that has been used for prediction. Whereas tumor control is the desired outcome from radiation targeting tumorous tissue, toxicity is the unwanted effects of radiation inevitably affecting surrounding normal tissue. Various applications have been applied to different sites of cancer. For example, Zhen *et al*[60] predicted rectum toxicity in cervical cancer using CNN, Ibragimov *et al*[70] predicted hepatobiliary toxicity after liver SBRT using CNN, and Valdes *et al*[71] predicted radiation pneumonitis after SBRT for stage I NSCLC using RUSBoost algorithm with regularization.

There have also been works that combine the outcomes of both the toxicity and the tumor response to RT. For example, Qi *et al*[72], applied a DNN to predict the patient reported quality of life in urinary and bowel symptoms, after SBRT for prostate cancer.

The model was trained on the dosimetry data alone. The urinary symptoms were predicted by the volume of the tumor, while the bowel symptoms represent the toxicity to the rectum.

HUMAN AI INTERACTION

As the use of AI technology progress, we need to examine the role of AI in conjunction with human. In the short term, this is likely to be in a collaborative/hybrid manner, rather AI operating autonomously, although this will depend on the tasks at hand. The impact of AI in the radiation oncology field is increasing rapidly, but at the same time the concern surrounding the use of AI is rising. One of the main concerns is the replacement of many jobs in the field of medical physics and radiation oncology, which can lead to a change in how patients are being treated. It is important to understand the perception of radiation oncology staff about the progression of AI and increase the awareness of the using of AI as a cooperative tool instead of job replacements. With the integration of AI in the profession, there is a huge potential in improving radiation oncology treatments and decision-making processes[73].

Limitations of AI

The efficiency and accuracy will be revolutionized by AI, but the future role of AI is not as clear, and the responsibility of the AI algorithm and clinicians using the AI needs to be addressed. In RT treatment planning, most plans are generated based on ground truth with low variability, but the optimization requires insights from clinicians to provide a creative solution for the patient. With the heavy reliance on technology, the innovative aspect may be reduced with the lack of human inputs. Safety risks such as AI being reluctant to highlight its own limitations are possible, with the potential of suboptimal plans being passed for treatment[74]. There is likely to be ongoing need of human/clinical oversight, not least due to regulatory requirements.

The concerns of using AI stem from the key issues surrounding the lack of empathy and intuition, unlike human practitioners. The development of empathy, which leads to the clinician focusing on the patients' well-being could play a subconscious role in providing a creative, innovative and safe RT treatment. This philosophical issue relates to human consciousness, and it contributes to how health practitioners should approach, use and interact with AI. The term preconceptual understanding, can be referred to as common sense for human in general. Since AI is perceived to not possess human common sense, it may affect its ability to perform certain tasks that require incorporation of these kinds of thinking[74].

Human cognition has two main attributes, which are concept and intuition. Human relies on these attributes to relate to the world and people around us. The concept of being affected by other people has an impact on how we behave towards them. Affectivity between individuals makes us take responsibility for other people, altering our behaviours either consciously or unconsciously. The intended consequence is generally thought to be that humans will behave in an ethical manner. In RT practice, clinical guidance exists for clinicians to follow and failure to act ethically would have serious consequences[74].

With the lack of intuition, AI may not behave with identical traits as human. The focus of the AI will be based on preprogrammed objectives, instead of patient outcomes and may even display a lack of creative input. Patient care and communication should be performed by human professionals because human needs to be involved in the RT routines, so the safety, creativity and innovation can be maintained. In the short term, the use of AI may assist treatment planning, potentially saving time. Clinicians will be required to integrate the technology into their practice, being aware of limitations, and how it can assist decision making. The unintended consequence may be that there are less opportunities or experience in training, and the training the future generation of medical staff for providing competent oversight may need to be addressed[74].

Karches[75] proposed that AI should not replace physician judgement. Technology should help us to extract things from their context, but when technological advancement leads us to reduce qualitative into quantitative information, eventually interactions between people could become mere data and information, driven to the point where only the quantifiable entities matter. Karches[75] mentioned two examples, which are stethoscopes and electronic health record (HER), to explain technologies can both help or hinder primary care. A stethoscope allows the

physicians to pay attention to the sounds of the patients' body functions. The physicians merely utilize a tool to increase their ability to extract information, the tool acts as an extension of the physician which still allows the physicians to conform their judgement to the patients' reality. However, EHR tends to distance the physician from the patient. A collection of fact is presented to the physicians before meeting the patient can surely make the examination process to be more efficient, but the lack of interaction between physician and patient can lead the physician to be less adapted to handle aspects of patient care that is not quantifiable by technology[75]. Limiting patient interaction also leads to less empathy and rapport, potentially leading to less trust in medical professionals.

They are unlikely to devote more time to uncompensated activities such as educating students[75]. These examples are an important reminder of how clinicians should interact with AI, where AI needs to be a tool to assist the clinicians to gain a better understanding of the patient and situation, but not something to distract themselves which compromise primary care. The more optimistic model of AI usage may be that AI frees the physicians or medical practitioners from repetitive or mundane, enabling them to spend more time with patients.

AI perception

Wong *et al* have surveyed the Canadian radiation oncology staff in 2020 regarding their views towards the impact of AI. Even though more than 90% of the respondents were interested in learning more about AI, only 12% of them felt they were knowledgeable about AI. For the forecast of AI, the majority of the respondents felt optimistic, and it would save time and benefit the patients. Common concerns among the staff were the economic implications and the lack of patient interaction. The precision of AI in identifying organs at risk is the top priority, and most concurred that AI system could produce better than average performance, but human oversight is still necessary for providing the best quality of patient care. Many respondents, especially radiation trainees, had concerns about AI could replace their professional responsibilities[73].

Medical practitioners have expressed frustration at the technologies because the relationship between the patient and medical staff are undermined. The AI produces a medical judgement, often disregarding the particular circumstances of each patient. This is because any extra consideration for the patient may lead to an increase in cost, lowering efficiency. Many experienced clinicians would not rely solely on the patients' verbal description because patients could be untruthful about their purpose of visit, or they might understate the burden of their symptoms. AI would tend to take the history of patients at face value, and depending on the technology used, it may never have the ability to interpret subtle non-verbal cues. The ability to understand the patients' needs remain questionable, as the best patient outcome does not always have a binary result which computers are good at producing[75].

The reduction of time-consuming tasks due to the AI integration may cause a reduction in job opportunities. On the other hand, the decrease in a more time-consuming task can lead to better inter-professional collaboration and an increase in interaction time with the patient. According to the survey from Wong *et al*[73], the cost benefits of AI was unclear for the respondents and it can be one of the reasons for the limitation on AI advancement. There could be a need for incorporating the knowledge of AI in the early stages of education, this is because the trainees which will be the future generation of practitioners, showed the least positivity towards AI. The fear of the unknown is part of human nature, and therefore, the investment of educating professionals to raise the knowledge and importance of AI is essential[73].

Techniques to improve human-AI interaction

Although AI has the potential to expand or extend beyond the cognitive abilities of humans, it still has its limitations in its current form that only humans can demonstrate such as generalisability and empathy. These limitations are especially pronounced in fields where data is limited and social context is paramount, such as in medicine and RT. There is an idea to create systems that combine humans and AI in symbiosis, with the intention that the whole is greater than the sum of its parts[76]. The ideal hybridized system would allow the two parties to combine the strengths yet hide the weaknesses of each other. However, the key to optimizing these systems is to have an efficient Human-AI interaction process. The interaction process has been subject to recent research. Design principles have been set forth, though applications within RT may be in its infancy.

To conceptualise the process of human-AI interaction, some groups have written guidelines and taxonomies for the design of such processes. Amershi *et al*[77] have created design guidelines for human-AI interaction, based on the feedback and experience of design practitioners. The focus is on a human-centric system with AI as an assistant. Key features can be divided over different time points of the interaction: (1) Before interaction (initiation): How does AI set expectations on its strengths and limitations? (2) On interaction: How does AI present information to a human? How does human provide feedback to AI? and (3) After interaction (over time): How does AI learn and adapt to human preferences?

The initiation phase occurs before any interaction occurs when expectations are set out for each other. Cai *et al*[78] have investigated what medical practitioners desired to know about the AI before using it. The requirements were akin to what the users desired to know about their human colleagues when consulting or cooperating with them. The properties of the AI can be described along these lines including its known strengths and limitations (*e.g.*, bias of training data), its functionality (*e.g.*, the task it was trained to perform), its objective (*e.g.*, was it designed to be sensitive or specific) and socioeconomic implications. With appropriate expectations set, the user may be motivated to adopt the system in various modes of collaboration. For example, the human-AI system can divide labour according to their strengths, or they can perform the same task as a second opinion to each other.

During the interaction, the AI and human communicate to share information. Firstly, there is a consideration of what information is to be shared. With current AI systems using deep learning, a decision or prediction is made based on given inputs. However, there is a common concern of interpretability of such decisions of AI systems because of the lack of explicit steps of reasoning between input and output. In order to gain trust in AI decision, interpretability or explanability has been a growing area in AI research in general. To this end, Luo *et al*[79] reviewed different AI algorithms with improved interpretability for RT outcome prediction. Some examples include using handcrafted features or activation maps. However, there is a trade-off between the algorithm's interpretability and its accuracy. Other methods include using SHAP analysis which is used to explain feature importance in tree-based models[80]. Secondly, there is a consideration of how to present the information in the workflow so that this integrates well in clinical practice. Ramkumar *et al*[81] explored the user interaction in semi-automatic segmentation of organs at risk. It was shown that the physicians' subjective preferences of different workflows play an important role, suggesting flexibility in system design needs to be bourne in mind. The experience and/or personal preference of an individual practitioner may also play a role. A recent study demonstrated that humans are susceptible to bias when given advice and this is particularly more pronounced with doctors with less experience on the task of chest radiograph interpretation[82]. Figure 5 shows the likely future direction of the development of AI and human-AI interaction. The incorporation of AI under human supervision will likely become mainstream in clinical practice in the future, until the AI has sufficient or near-human consciousness to perform tasks autonomously. In between, there may also be a hybrid mode of operation, whereby a direct interface with human may be used. For example, there are developments to implant chips in human brain so that we can directly interface with a computer system. This mode of operation could be used for example, for real-time adjustment in treatment plan during treatment delivery.

CONCLUSION

The examples of applications and potential of AI provide insights on how and why health care professionals such as medical physicists and radiation oncologists should use AI. The pros and cons with AI usage needs to be understood fully in order to both strengthen our ability to provide primary care and reduce the amount of weaknesses that human and AI possess.

The role of medical physicists will likely migrate away from QA of equipment, towards the QA of the patient treatments and overall treatment environment and processes. The decision-making capacity is expected to be improved and the knowledge gaps between experts and non-experts of a specific domain may be lowered. Clinicians are going to interact with computers more often and the efficiency of the human-computer interface will play a larger role in reducing duplicative and manual efforts. With the advancement of AI in the near future, the performance may, if not already, have surpassed human in specific tasks. It is crucial to re-think the

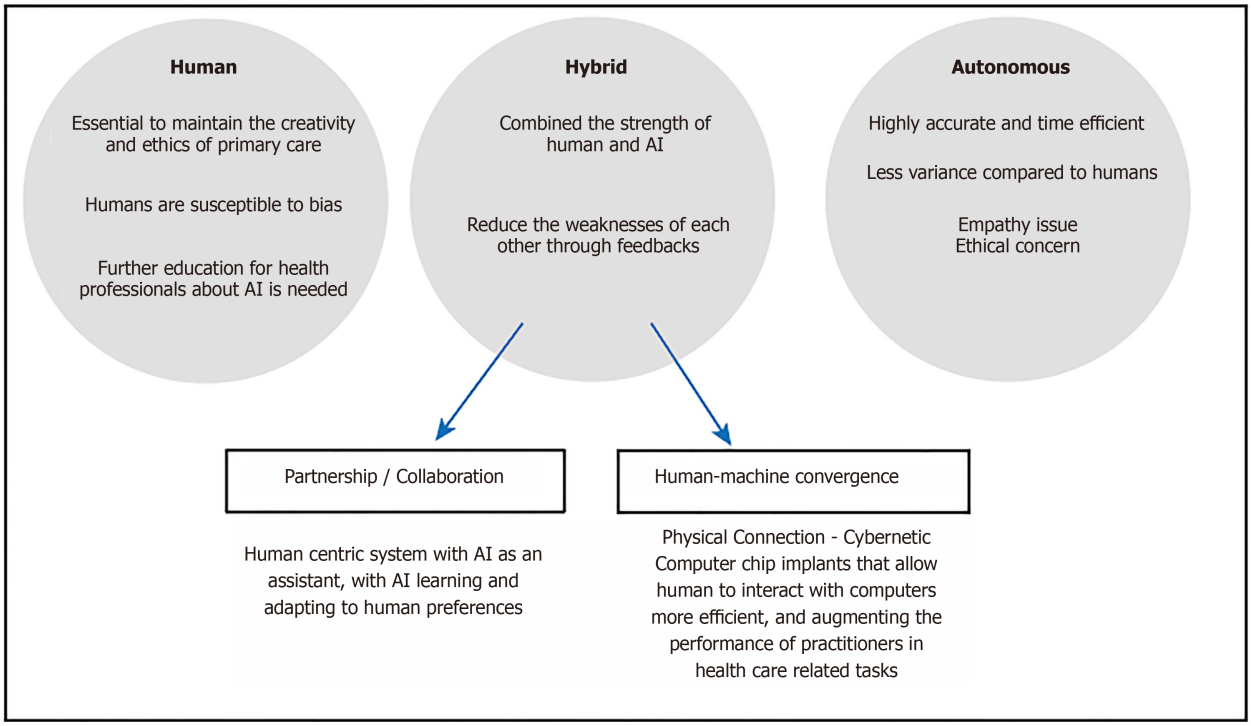

Figure 5 Future direction of human and artificial Intelligence. AI: Artificial intelligence.

ethical clinical practice, when do we decide to let a human make a "correction" to the output provided by an AI[2], or when can we allow AI system to operate autonomously.

The growth of AI also poses security challenges as the data are shared more often across governance structures and stakeholders. Implications of unintended third-party data reuse may be more common. As a consequent, already there are some efforts such as the increased requirements of European Union's General Data Protection Regulation to reduce the concern of the breach in privacy. Early AI that is clinically adopted might have flaws that result in patient harm just as some early IMRT systems. Nevertheless, AI will one day become widespread and effective technology[2].

Despite the potential drawbacks, the enormous benefit provided by AI will allow medical practitioners to provide a better healthcare service to patients. In the previous sections of this review, many techniques are currently in research. The clinical practice will be adopting the use of AI more in the future, and the examples listed above will likely become available and applied within the next decade.

While we are still a long way from having fully autonomous AI to determine the best treatment options, steps were taken in this direction such as improving AI algorithms through trainings and feedbacks. In the short term, there are likely to be some changes in the working environment. It would be foolhardy to expect that we maintain the status quo. Although medical practitioners are unlikely to be replaced any time soon, we expect the profession to evolve. Displacement of practitioner's roles rather than replacement may be the impact in the foreseeable future.

REFERENCES

1 **Siddique S**, Chow JCL. Artificial intelligence in radiotherapy. *Rep Pract Oncol Radiother* 2020; **25**: 656-666 [PMID: 32617080 DOI: 10.1016/j.rpor.2020.03.015]

2 **Thompson RF**, Valdes G, Fuller CD, Carpenter CM, Morin O, Aneja S, Lindsay WD, Aerts HJWL, Agrimson B, Deville C Jr, Rosenthal SA, Yu JB, Thomas CR Jr. Artificial intelligence in radiation oncology: A specialty-wide disruptive transformation? *Radiother Oncol* 2018; **129**: 421-426 [PMID: 29907338 DOI: 10.1016/j.radonc.2018.05.030]

3 **Meyer P**, Noblet V, Mazzara C, Lallement A. Survey on deep learning for radiotherapy. *Comput Biol Med* 2018; **98**: 126-146 [PMID: 29787940 DOI: 10.1016/j.compbiomed.2018.05.018]

4 **Wang T**, Lei Y, Fu Y, Wynne JF, Curran WJ, Liu T, Yang X. A review on medical imaging synthesis using deep learning and its clinical applications. *J Appl Clin Med Phys* 2021; **22**: 11-36 [PMID: 33305538 DOI: 10.1002/acm2.13121]

5 **Fu Y**, Lei Y, Zhou J, Wang T, Yu DS, Beitler JJ, Curran WJ; Liu T, Yang, X. Synthetic CT-aided MRI-CT image registration for head and neck radiotherapy. In: Gimi BS, Krol A. Medical Imaging 2020: Biomedical Applications in Molecular, Structural, and Functional Imaging. SPIE, 2020: 77 [DOI: 10.1117/12.2549092]

6 **Liu Y**, Lei Y, Wang T, Kayode O, Tian S, Liu T, Patel P, Curran WJ, Ren L, Yang X. MRI-based treatment planning for liver stereotactic body radiotherapy: validation of a deep learning-based synthetic CT generation method. *Br J Radiol* 2019; **92**: 20190067 [PMID: 31192695 DOI: 10.1259/bjr.20190067]

7 **Liu Y**, Lei Y, Wang Y, Shafai-Erfani G, Wang T, Tian S, Patel P, Jani AB, McDonald M, Curran WJ, Liu T, Zhou J, Yang X. Evaluation of a deep learning-based pelvic synthetic CT generation technique for MRI-based prostate proton treatment planning. *Phys Med Biol* 2019; **64**: 205022 [PMID: 31487698 DOI: 10.1088/1361-6560/ab41af]

8 **Lei Y**, Dong X, Tian Z, Liu Y, Tian S, Wang T, Jiang X, Patel P, Jani AB, Mao H, Curran WJ, Liu T, Yang X. CT prostate segmentation based on synthetic MRI-aided deep attention fully convolution network. *Med Phys* 2020; **47**: 530-540 [PMID: 31745995 DOI: 10.1002/mp.13933]

9 **Dong C**, Loy CC, He K, Tang X. Image Super-Resolution Using Deep Convolutional Networks. *IEEE Trans Pattern Anal Mach Intell* 2016; **38**: 295-307 [PMID: 26761735 DOI: 10.1109/TPAMI.2015.2439281]

10 **Bahrami K**, Shi F, Rekik I, Shen D. Convolutional neural network for reconstruction of 7T-like images from 3T MRI using appearance and anatomical features. In: Carneiro G, Mateus D, Peter L, Bradley A, Tavares JMRS, Belagiannis V, Papa JP, Nascimento JC, Loog M, Lu Z, Cardoso JS, Cornebise J. Deep Learning and Data Labeling for Medical Applications. DLMIA 2016, LABELS 2016. Lecture Notes in Computer Science, vol 10008. Cham: Springer, 2016: 39-47 [DOI: 10.1007/978-3-319-46976-8_5]

11 **Qu L**, Zhang Y, Wang S, Yap PT, Shen D. Synthesized 7T MRI from 3T MRI *via* deep learning in spatial and wavelet domains. *Med Image Anal* 2020; **62**: 101663 [PMID: 32120269 DOI: 10.1016/j.media.2020.101663]

12 **Yang Q**, Yan P, Zhang Y, Yu H, Shi Y, Mou X, Kalra MK, Sun L, Wang G. Low-Dose CT Image Denoising Using a Generative Adversarial Network With Wasserstein Distance and Perceptual Loss. *IEEE Trans Med Imaging* 2018; **37**: 1348-1357 [PMID: 29870364 DOI: 10.1109/TMI.2018.2827462]

13 **Wang T**, Lei Y, Tian Z, Dong X, Liu Y, Jiang X, Curran WJ, Liu T, Shu HK, Yang X. Deep learning-based image quality improvement for low-dose computed tomography simulation in radiation therapy. *J Med Imaging (Bellingham)* 2019; **6**: 043504 [PMID: 31673567 DOI: 10.1117/1.JMI.6.4.043504]

14 **Chen H**, Zhang Y, Zhang W, Liao P, Li K, Zhou J, Wang G. Low-dose CT *via* convolutional neural network. *Biomed Opt Express* 2017; **8**: 679-694 [PMID: 28270976 DOI: 10.1364/BOE.8.000679]

15 **Cardenas CE**, Yang J, Anderson BM, Court LE, Brock KB. Advances in Auto-Segmentation. *Semin Radiat Oncol* 2019; **29**: 185-197 [PMID: 31027636 DOI: 10.1016/j.semradonc.2019.02.001]

16 **Zhou SK**, Greenspan H, Shen D. Deep Learning for Medical Image Analysis. 1st ed. San Diego: Elsevier, 2017

17 **Krizhevsky A**, Sutskever I, Hinton GE. ImageNet classification with deep convolutional neural networks. In: Bartlett P, Pereira PCN, Burges CJC, Bottou L, Weinberger KQ. Advances in Neural Information Processing Systems 25. Curran Associates, 2012

18 **Ibragimov B**, Toesca D, Chang D, Koong A, Xing L. Combining deep learning with anatomical analysis for segmentation of the portal vein for liver SBRT planning. *Phys Med Biol* 2017; **62**: 8943-8958 [PMID: 28994665 DOI: 10.1088/1361-6560/aa9262]

19 **Li W**, Jia F, Hu Q. Automatic Segmentation of Liver Tumor in CT Images with Deep Convolutional Neural Networks. *J Comput Commun* 2015; **3**: 146-151 [DOI: 10.4236/jcc.2015.311023]

20 **Chen LC**, Papandreou G, Schroff F, Adam H. Rethinking atrous convolution for semantic image segmentation. 2017 Preprint. Available from: arXiv:1706.05587

21 **Ronneberger O**, Fischer P, Brox T. U-net: Convolutional networks for biomedical image segmentation. In: Navab N, Hornegger J, Wells W, Frangi A. Medical Image Computing and Computer-Assisted Intervention – MICCAI 2015. MICCAI 2015. Lecture Notes in Computer Science, vol 9351. Cham: Springer, 2015: 234-241 [DOI: 10.1007/978-3-319-24574-4_28]

22 **Shelhamer E**, Long J, Darrell T. Fully Convolutional Networks for Semantic Segmentation. *IEEE Trans Pattern Anal Mach Intell* 2017; **39**: 640-651 [PMID: 27244717 DOI: 10.1109/TPAMI.2016.2572683]

23 **Qayyum A**, Ahmad I, Mumtaz W, Alassafi MO, Alghamdi R, Mazher M. Automatic Segmentation Using a Hybrid Dense Network Integrated With an 3D-Atrous Spatial Pyramid Pooling Module for Computed Tomography (CT) Imaging. *IEEE Access* 2020; **8**: 169794-169803 [DOI: 10.1109/access.2020.3024277]

24 **Clark K**, Vendt B, Smith K, Freymann J, Kirby J, Koppel P, Moore S, Phillips S, Maffitt D, Pringle M, Tarbox L, Prior F. Browse Data Collections. The Cancer Imaging Archive (TCIA), 2021

25 **Freimuth M**. NIH Clinical Center releases dataset of 32,000 CT images. National Institutes of Health, US. Available from: https://www.nih.gov/news-events/news-releases/nih-clinical-center-releases-dataset-32000-ct-images

26 **University of Southern California**. Medical imaging data archived in the IDA. Available from: https://ida.loni.usc.edu/services/Menu/IdaData.jsp?project=

27 **Jiang D**, Yan H, Chang N, Li T, Mao R, Du C, Guo B, Liu J. Convolutional neural network-based dosimetry evaluation of esophageal radiation treatment planning. *Med Phys* 2020; **47**: 4735-4742 [PMID: 32767840 DOI: 10.1002/mp.14434]

28 **Nawa K**, Haga A, Nomoto A, Sarmiento RA, Shiraishi K, Yamashita H, Nakagawa K. Evaluation of a commercial automatic treatment planning system for prostate cancers. *Med Dosim* 2017; **42**: 203-209 [PMID: 28549556 DOI: 10.1016/j.meddos.2017.03.004]

29 **Krayenbuehl J**, Zamburlini M, Ghandour S, Pachoud M, Tanadini-Lang S, Tol J, Guckenberger M, Verbakel WFAR. Planning comparison of five automated treatment planning solutions for locally advanced head and neck cancer. *Radiat Oncol* 2018; **13**: 170 [PMID: 30201017 DOI: 10.1186/s13014-018-1113-z]

30 **Nelms BE**, Robinson G, Markham J, Velasco K, Boyd S, Narayan S, Wheeler J, Sobczak ML. Variation in external beam treatment plan quality: An inter-institutional study of planners and planning systems. *Pract Radiat Oncol* 2012; **2**: 296-305 [PMID: 24674168 DOI: 10.1016/j.prro.2011.11.012]

31 **Batumalai V**, Jameson MG, Forstner DF, Vial P, Holloway LC. How important is dosimetrist experience for intensity modulated radiation therapy? *Pract Radiat Oncol* 2013; **3**: e99-e106 [PMID: 24674377 DOI: 10.1016/j.prro.2012.06.009]

32 **Hazell I**, Bzdusek K, Kumar P, Hansen CR, Bertelsen A, Eriksen JG, Johansen J, Brink C. Automatic planning of head and neck treatment plans. *J Appl Clin Med Phys* 2016; **17**: 272-282 [PMID: 26894364 DOI: 10.1120/jacmp.v17i1.5901]

33 **Kida S**, Nakamoto T, Nakano M, Nawa K, Haga A, Kotoku J, Yamashita H, Nakagawa K. Cone Beam Computed Tomography Image Quality Improvement Using a Deep Convolutional Neural Network. *Cureus* 2018; **10**: e2548 [PMID: 29963342 DOI: 10.7759/cureus.2548]

34 **Huynh E**, Hosny A, Guthier C, Bitterman DS, Petit SF, Haas-Kogan DA, Kann B, Aerts HJWL, Mak RH. Artificial intelligence in radiation oncology. *Nat Rev Clin Oncol* 2020; **17**: 771-781 [PMID: 32843739 DOI: 10.1038/s41571-020-0417-8]

35 **Langen KM**, Jones DT. Organ motion and its management. *Int J Radiat Oncol Biol Phys* 2001; **50**: 265-278 [PMID: 11316572 DOI: 10.1016/S0360-3016(01)01453-5]

36 **Murphy MJ**, Pokhrel D. Optimization of an adaptive neural network to predict breathing. *Med Phys* 2009; **36**: 40-47 [PMID: 19235372 DOI: 10.1118/1.3026608]

37 **Isaksson M**, Jalden J, Murphy MJ. On using an adaptive neural network to predict lung tumor motion during respiration for radiotherapy applications. *Med Phys* 2005; **32**: 3801-3809 [PMID: 16475780 DOI: 10.1118/1.2134958]

38 **Ménard C**, Paulson E, Nyholm T, McLaughlin P, Liney G, Dirix P, van der Heide UA. Role of Prostate MR Imaging in Radiation Oncology. *Radiol Clin North Am* 2018; **56**: 319-325 [PMID: 29420985 DOI: 10.1016/j.rcl.2017.10.012]

39 **Wegener D**, Zips D, Thorwarth D, Weiß J, Othman AE, Grosse U, Notohamiprodjo M, Nikolaou K, Müller AC. Precision of T2 TSE MRI-CT-image fusions based on gold fiducials and repetitive T2 TSE MRI-MRI-fusions for adaptive IGRT of prostate cancer by using phantom and patient data. *Acta Oncol* 2019; **58**: 88-94 [PMID: 30264629 DOI: 10.1080/0284186X.2018.1518594]

40 **Gustafsson CJ**, Swärd J, Adalbjörnsson SI, Jakobsson A, Olsson LE. Development and evaluation of a deep learning based artificial intelligence for automatic identification of gold fiducial markers in an MRI-only prostate radiotherapy workflow. *Phys Med Biol* 2020; **65**: 225011 [PMID: 33179610 DOI: 10.1088/1361-6560/abb0f9]

41 **Persson E**, Jamtheim Gustafsson C, Ambolt P, Engelholm S, Ceberg S, Bäck S, Olsson LE, Gunnlaugsson A. MR-PROTECT: Clinical feasibility of a prostate MRI-only radiotherapy treatment workflow and investigation of acceptance criteria. *Radiat Oncol* 2020; **15**: 77 [PMID: 32272943 DOI: 10.1186/s13014-020-01513-7]

42 **Unkelbach J**, Bortfeld T, Craft D, Alber M, Bangert M, Bokrantz R, Chen D, Li R, Xing L, Men C, Nill S, Papp D, Romeijn E, Salari E. Optimization approaches to volumetric modulated arc therapy planning. *Med Phys* 2015; **42**: 1367-1377 [PMID: 25735291 DOI: 10.1118/1.4908224]

43 **Bohoudi O**, Bruynzeel AME, Senan S, Cuijpers JP, Slotman BJ, Lagerwaard FJ, Palacios MA. Fast and robust online adaptive planning in stereotactic MR-guided adaptive radiation therapy (SMART) for pancreatic cancer. *Radiother Oncol* 2017; **125**: 439-444 [PMID: 28811038 DOI: 10.1016/j.radonc.2017.07.028]

44 **Lamb J**, Cao M, Kishan A, Agazaryan N, Thomas DH, Shaverdian N, Yang Y, Ray S, Low DA, Raldow A, Steinberg ML, Lee P. Online Adaptive Radiation Therapy: Implementation of a New Process of Care. *Cureus* 2017; **9**: e1618 [PMID: 29104835 DOI: 10.7759/cureus.1618]

45 **Hrinivich WT**, Lee J. Artificial intelligence-based radiotherapy machine parameter optimization using reinforcement learning. *Med Phys* 2020; **47**: 6140-6150 [PMID: 33070336 DOI: 10.1002/mp.14544]

46 **Debus C**, Oelfke U, Bartzsch S. A point kernel algorithm for microbeam radiation therapy. *Phys Med Biol* 2017; **62**: 8341-8359 [PMID: 28922140 DOI: 10.1088/1361-6560/aa8d63]

47 **Bangert M**, Oelfke U. Spherical cluster analysis for beam angle optimization in intensity-modulated radiation therapy treatment planning. *Phys Med Biol* 2010; **55**: 6023-6037 [PMID: 20858916 DOI: 10.1088/0031-9155/55/19/025]

48 **Zhang X**, Homma N, Ichiji K, Abe M, Sugita N, Takai Y, Narita Y, Yoshizawa M. A kernel-based method for markerless tumor tracking in kV fluoroscopic images. *Phys Med Biol* 2014; **59**: 4897-4911 [PMID: 25098382 DOI: 10.1088/0031-9155/59/17/4897]

49 **Zhao W**, Han B, Yang Y, Buyyounouski M, Hancock SL, Bagshaw H, Xing L. Incorporating imaging information from deep neural network layers into image guided radiation therapy (IGRT). *Radiother Oncol* 2019; **140**: 167-174 [PMID: 31302347 DOI: 10.1016/j.radonc.2019.06.027]

50 **Kalet AM**, Luk SMH, Phillips MH. Radiation Therapy Quality Assurance Tasks and Tools: The Many Roles of Machine Learning. *Med Phys* 2020; **47**: e168-e177 [PMID: 30768796 DOI: 10.1002/mp.13445]

51 **Vandewinckele L**, Claessens M, Dinkla A, Brouwer C, Crijns W, Verellen D, van Elmpt W. Overview of artificial intelligence-based applications in radiotherapy: Recommendations for implementation and quality assurance. *Radiother Oncol* 2020; **153**: 55-66 [PMID: 32920005 DOI: 10.1016/j.radonc.2020.09.008]

52 **Chang X**, Li H, Kalet A, Yang D. Detecting External Beam Radiation Therapy Physician Order Errors Using Machine Learning. *Int J Radiat Oncol* 2017; **99**: S71 [DOI: 10.1016/j.ijrobp.2017.06.174]

53 **Kalet AM**, Gennari JH, Ford EC, Phillips MH. Bayesian network models for error detection in radiotherapy plans. *Phys Med Biol* 2015; **60**: 2735-2749 [PMID: 25768885 DOI: 10.1088/0031-9155/60/7/2735]

54 **Tomori S**, Kadoya N, Takayama Y, Kajikawa T, Shima K, Narazaki K, Jingu K. A deep learning-based prediction model for gamma evaluation in patient-specific quality assurance. *Med Phys* 2018 [PMID: 30066388 DOI: 10.1002/mp.13112]

55 **Nyflot MJ**, Thammasorn P, Wootton LS, Ford EC, Chaovalitwongse WA. Deep learning for patient-specific quality assurance: Identifying errors in radiotherapy delivery by radiomic analysis of gamma images with convolutional neural networks. *Med Phys* 2019; **46**: 456-464 [PMID: 30548601 DOI: 10.1002/mp.13338]

56 **Granville DA**, Sutherland JG, Belec JG, La Russa DJ. Predicting VMAT patient-specific QA results using a support vector classifier trained on treatment plan characteristics and linac QC metrics. *Phys Med Biol* 2019; **64**: 095017 [PMID: 30921785 DOI: 10.1088/1361-6560/ab142e]

57 **Li Q**, Chan MF. Predictive time-series modeling using artificial neural networks for Linac beam symmetry: an empirical study. *Ann N Y Acad Sci* 2017; **1387**: 84-94 [PMID: 27627049 DOI: 10.1111/nyas.13215]

58 **Xu Y**, Hosny A, Zeleznik R, Parmar C, Coroller T, Franco I, Mak RH, Aerts HJWL. Deep Learning Predicts Lung Cancer Treatment Response from Serial Medical Imaging. *Clin Cancer Res* 2019; **25**: 3266-3275 [PMID: 31010833 DOI: 10.1158/1078-0432.CCR-18-2495]

59 **Shi L**, Zhang Y, Nie K, Sun X, Niu T, Yue N, Kwong T, Chang P, Chow D, Chen JH, Su MY. Machine learning for prediction of chemoradiation therapy response in rectal cancer using pre-treatment and mid-radiation multi-parametric MRI. *Magn Reson Imaging* 2019; **61**: 33-40 [PMID: 31059768 DOI: 10.1016/j.mri.2019.05.003]

60 **Zhen X**, Chen J, Zhong Z, Hrycushko B, Zhou L, Jiang S, Albuquerque K, Gu X. Deep convolutional neural network with transfer learning for rectum toxicity prediction in cervical cancer radiotherapy: a feasibility study. *Phys Med Biol* 2017; **62**: 8246-8263 [PMID: 28914611 DOI: 10.1088/1361-6560/aa8d09]

61 **Mizutani T**, Magome T, Igaki H, Haga A, Nawa K, Sekiya N, Nakagawa K. Optimization of treatment strategy by using a machine learning model to predict survival time of patients with malignant glioma after radiotherapy. *J Radiat Res* 2019; **60**: 818-824 [PMID: 31665445 DOI: 10.1093/jrr/rrz066]

62 **Oikonomou A**, Khalvati F, Tyrrell PN, Haider MA, Tarique U, Jimenez-Juan L, Tjong MC, Poon I, Eilaghi A, Ehrlich L, Cheung P. Radiomics analysis at PET/CT contributes to prognosis of recurrence and survival in lung cancer treated with stereotactic body radiotherapy. *Sci Rep* 2018; **8**: 4003 [PMID: 29507399 DOI: 10.1038/s41598-018-22357-y]

63 **Aneja S**, Shaham U, Kumar RJ, Pirakitikulr N, Nath SK, Yu JB, Carlson DJ, Decker RH. Deep Neural Network to Predict Local Failure Following Stereotactic Body Radiation Therapy: Integrating Imaging and Clinical Data to Predict Outcomes. *Int J Radiat Oncol* 2017; **99**: S47 [DOI: 10.1016/j.ijrobp.2017.06.120]

64 **Zhou Z**, Folkert M, Cannon N, Iyengar P, Westover K, Zhang Y, Choy H, Timmerman R, Yan J, Xie XJ, Jiang S, Wang J. Predicting distant failure in early stage NSCLC treated with SBRT using clinical parameters. *Radiother Oncol* 2016; **119**: 501-504 [PMID: 27156652 DOI: 10.1016/j.radonc.2016.04.029]

65 **Wang C**, Rimner A, Hu YC, Tyagi N, Jiang J, Yorke E, Riyahi S, Mageras G, Deasy JO, Zhang P. Toward predicting the evolution of lung tumors during radiotherapy observed on a longitudinal MR imaging study *via* a deep learning algorithm. *Med Phys* 2019; **46**: 4699-4707 [PMID: 31410855 DOI: 10.1002/mp.13765]

66 **Tseng HH**, Luo Y, Cui S, Chien JT, Ten Haken RK, Naqa IE. Deep reinforcement learning for automated radiation adaptation in lung cancer. *Med Phys* 2017; **44**: 6690-6705 [PMID: 29034482 DOI: 10.1002/mp.12625]

67 **Hu Y**, Xie C, Yang H, Ho JWK, Wen J, Han L, Lam KO, Wong IYH, Law SYK, Chiu KWH, Vardhanabhuti V, Fu J. Computed tomography-based deep-learning prediction of neoadjuvant chemoradiotherapy treatment response in esophageal squamous cell carcinoma. *Radiother Oncol* 2021; **154**: 6-13 [PMID: 32941954 DOI: 10.1016/j.radonc.2020.09.014]

68 **Hu Y**, Xie C, Yang H, Ho JWK, Wen J, Han L, Chiu KWH, Fu J, Vardhanabhuti V. Assessment of Intratumoral and Peritumoral Computed Tomography Radiomics for Predicting Pathological Complete Response to Neoadjuvant Chemoradiation in Patients With Esophageal Squamous Cell

Carcinoma. *JAMA Netw Open* 2020; **3**: e2015927 [PMID: 32910196 DOI: 10.1001/jamanetworkopen.2020.15927]

69 **Du R**, Lee VH, Yuan H, Lam KO, Pang HH, Chen Y, Lam EY, Khong PL, Lee AW, Kwong DL, Vardhanabhuti V. Radiomics Model to Predict Early Progression of Nonmetastatic Nasopharyngeal Carcinoma after Intensity Modulation Radiation Therapy: A Multicenter Study. *Radiol Artif Intell* 2019; **1**: e180075 [DOI: 10.1148/ryai.2019180075]

70 **Ibragimov B**, Toesca D, Chang D, Yuan Y, Koong A, Xing L. Development of deep neural network for individualized hepatobiliary toxicity prediction after liver SBRT. *Med Phys* 2018; **45**: 4763-4774 [PMID: 30098025 DOI: 10.1002/mp.13122]

71 **Valdes G**, Solberg TD, Heskel M, Ungar L, Simone CB 2nd. Using machine learning to predict radiation pneumonitis in patients with stage I non-small cell lung cancer treated with stereotactic body radiation therapy. *Phys Med Biol* 2016; **61**: 6105-6120 [PMID: 27461154 DOI: 10.1088/0031-9155/61/16/6105]

72 **Qi X**, Neylon J, Santhanam A. Dosimetric Predictors for Quality of Life After Prostate Stereotactic Body Radiation Therapy *via* Deep Learning Network. *Int J Radiat Oncol* 2017; **99**: S167 [DOI: 10.1016/j.ijrobp.2017.06.384]

73 **Wong K**, Gallant F, Szumacher E. Perceptions of Canadian radiation oncologists, radiation physicists, radiation therapists and radiation trainees about the impact of artificial intelligence in radiation oncology - national survey. *J Med Imaging Radiat Sci* 2021; **52**: 44-48 [PMID: 33323332 DOI: 10.1016/j.jmir.2020.11.013]

74 **Bridge P**, Bridge R. Artificial Intelligence in Radiotherapy: A Philosophical Perspective. *J Med Imaging Radiat Sci* 2019; **50**: S27-S31 [PMID: 31591033 DOI: 10.1016/j.jmir.2019.09.003]

75 **Karches KE**. Against the iDoctor: why artificial intelligence should not replace physician judgment. *Theor Med Bioeth* 2018; **39**: 91-110 [PMID: 29992371 DOI: 10.1007/s11017-018-9442-3]

76 **Jarrahi MH**. Artificial intelligence and the future of work: Human-AI symbiosis in organizational decision making. *Bus Horiz* 2018; **61**: 577-586 [DOI: 10.1016/j.bushor.2018.03.007]

77 **Amershi S**, Weld D, Vorvoreanu M, Fourney A, Nushi B, Collisson P, Suh J, Iqbal S, Bennett PN, Inkpen K, Teevan J, Kikin-Gil R, Horvitz E. Guidelines for human-AI interaction. In: CHI '19: Proceedings of the 2019 CHI Conference on Human Factors in Computing Systems; 2019 May 4-9; Glasgow Scotland; UK. New York: Association for Computing Machinery, 2019: 1-13 [DOI: 10.1145/3290605.3300233]

78 **Cai CJ**, Winter S, Steiner D, Wilcox L, Terry M. "Hello AI": Uncovering the onboarding needs of medical practitioners for human–AI collaborative decision-making. *Proc ACM Hum Comput Interact* 2019; **3**: 104 [DOI: 10.1145/3359206]

79 **Luo Y**, Tseng HH, Cui S, Wei L, Ten Haken RK, El Naqa I. Balancing accuracy and interpretability of machine learning approaches for radiation treatment outcomes modeling. *BJR Open* 2019; **1**: 20190021 [PMID: 33178948 DOI: 10.1259/bjro.20190021]

80 **Lundberg SM**, Lee SI. A unified approach to interpreting model predictions. In: Guyon I, Luxburg UV, Bengio S, Wallach H, Fergus R, Vishwanathan S, Garnett R, editors. Advances in Neural Information Processing Systems 30. Curran Associates, 2017

81 **Ramkumar A**, Dolz J, Kirisli HA, Adebahr S, Schimek-Jasch T, Nestle U, Massoptier L, Varga E, Stappers PJ, Niessen WJ, Song Y. User Interaction in Semi-Automatic Segmentation of Organs at Risk: a Case Study in Radiotherapy. *J Digit Imaging* 2016; **29**: 264-277 [PMID: 26553109 DOI: 10.1007/s10278-015-9839-8]

82 **Gaube S**, Suresh H, Raue M, Merritt A, Berkowitz SJ, Lermer E, Coughlin JF, Guttag JV, Colak E, Ghassemi M. Do as AI say: susceptibility in deployment of clinical decision-aids. *NPJ Digit Med* 2021; **4**: 31 [PMID: 33608629 DOI: 10.1038/s41746-021-00385-9]

Published by **Baishideng Publishing Group Inc**
7041 Koll Center Parkway, Suite 160, Pleasanton, CA 94566, USA
Telephone: +1-925-3991568
E-mail: bpgoffice@wjgnet.com
Help Desk: https://www.f6publishing.com/helpdesk
https://www.wjgnet.com

© 2021 Baishideng Publishing Group Inc. All rights reserved.